

# **Study The Effect of Surfactant on The Porous Structure of Silica Monolith**

**A**

**Dissertation submitted**

**In the partial fulfillment of the requirements for the degree of**

**M.Sc. (Chemistry)**



**Submitted by  
Pallavi Jain  
(301402013)**

**Under the Supervision of:**

**Dr. Soumen Basu  
Assistant Professor**

**School of Chemistry & Biochemistry,**

**Thapar University, Patiala-147004**

**July 2016**

## Certificate

This is to certify that the dissertation entitled, "**Study the effect of Surfactant on the Porous Structure of Silica Monolith**" being submitted by **Ms. Pallavi Jain** in partial fulfilment of the requirements for the award of degree of Master of Science in Chemistry and being submitted to the School of Chemistry and Biochemistry, Thapar University, Patiala, is a bonafide work carried out by her under our supervision. The work has reached the standard necessary for submission. The contents of this dissertation have not been submitted for the award of any other degree or diploma.

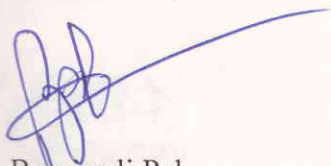


**Dr. Soumen Basu**

**Assistant Professor,**

**School of Chemistry & Biochemistry,**

**Thapar University, Patiala – 147 004**

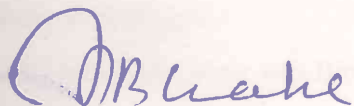


**Dr. Bonamali Pal**

**Head & Professor,**

**School of Chemistry and Biochemistry,**

**Thapar University, Patiala – 147 004**



**Dean of Academic Affairs**

**Thapar University, Patiala – 147 004**

## Candidate's Declaration

I hereby declare that the work being presented in the dissertation entitled “**Study the effect of Surfactant on the Porous Structure of Silica Monolith**” in partial fulfilment of the requirements for the award of degree of Masters of Science in Chemistry and being submitted to School of Chemistry and Biochemistry, Thapar University, Patiala, is my own work during the period of January to July 2016, under the supervision of **Dr. Soumen Basu**. I have not submitted the contents embodied in this dissertation for the award of any other degree.

**Patiala**

  
**Pallavi Jain**

**Date:** 28/6/16

This is to certify that the statement made by the candidate is correct and true to the best of our knowledge.



**Dr. Soumen Basu**

**Assistant Professor,**

**School of Chemistry & Biochemistry,**

**Thapar University, Patiala – 147 004**

  
**Dr. Bonamali Pal**

**Head & Professor,**

**School of Chemistry and Biochemistry,**

**Thapar University, Patiala – 147 004**

## Acknowledgment

First of all, I owe my gratitude to the Head of the Department, **Dr. Bonamali Pal** for providing me an opportunity in the form of this dissertation to develop my interest in research.

In the same spirit, I would like to thank my Supervisor, **Dr. Soumen Basu** for his constructive guidance and constant support during the project. The work presented here could not have been accomplished without their patience and ever willingness to teach. They have taught me to be concise and correct in my approach from the formulation of ideas to the presentation of the results.

Special thanks to all the **Teaching Faculty** of the department for their cooperation and guidance.

I would also like to express my gratitude to **Ms. Akansha Mehta, Mr. Amit Mishra, and Ms. Manisha Sharma** who never turned me down whenever I approached them for any kind of help. My heartfelt thanks to all the research scholars for their assistance.

I am grateful to **Thapar University & School of chemistry and biochemistry** for providing financial support and all necessary infrastructure and laboratory facilities to carry out the experimental work.

Words fail me to express my thanks to my family and friends who have always supported me and have been a source of strength and inspiration to me during the entire period of the work.

All these thanks are, however, only fraction of what is due to almighty for granting me an opportunity and strength to successfully accomplish this project.

Date: 28/6/16

  
Pallavi Jain

## **Abstract**

Sol-gel technique was used to fabricate silica monoliths by using different ratio of cationic, non-ionic and anionic surfactant which are used as moulds for various industrial applications. The as synthesized silica monoliths exhibits a hierarchical pore structure with inter-connected mesopores having pore diameter in the range 2-50nm which was confirmed by BET analysis. Further, the specific surface area was higher for monolith which was prepared by using cationic surfactant (C<sub>18</sub>TAB, 782.54) and the surface morphology was confirmed by SEM analysis. The results show the improvement of higher specific surface area of monoliths with different chain lengths of surfactants and with the increase in the surfactants concentrations.

## **List of Figures**

**Figure 1.1** - Types of nanoporous materials

**Figure 1.2** – Application of Nanoporous materials

**Figure 1.3** – Rock Stone Monolith

**Figure 1.4** –Application of monoliths

**Figure 1.5** - Monoliths

**Figure 1.6** - IUPAC classification of gas adsorption isotherms

**Figure 1.7** - BET Surface Analyser

**Figure 1.8** - SEM Analyser

**Figure 2.1** - Photograph of monoliths of different shapes exhibiting multimodal hierarchical porosity. The diameter of the coin is 23 mm.

**Figure 2.2** - SEM image of a macroporous sample (Magnification) 1000, scale bar) 20  $\mu$ m.

**Figure 2.3** - Pore size distribution of the Sample.

**Figure 3.1** - Structure of Trimethylstearylammoniumbromide ( $C_{18}TAB$ )

**Figure 3.2** - Synthesis of Surfactant solution on magnetic stirrer

**Figure 3.3** - Sartorius Weighing Balance

**Figure 3.4** - Hot Air Oven

**Figure 3.5** - Muffle Furnace

**Figure 3.6** - General steps involved in the production of silica monolith.

**Figure 3.7** – Mixing

**Figure 3.8** - Casting process

**Figure 3.9** - Gelation of monolith

**Figure 3.10** - Different monoliths formed by Sol-Gel Process.

**Figure 4.1** - The nitrogen adsorption-desorption isotherm for the  $SiO_2$  monoliths with different surfactant.

**Figure 4.2** - Pore size distributions for the SiO<sub>2</sub> monolith with different surfactants

**Figure 4.3** - Graph between type of surfactant and surface area.

**Figure 4.4** - The nitrogen adsorption-desorption isotherm for the SiO<sub>2</sub> monoliths with different C<sub>18</sub>TAB surfactant concentration.

**Figure 4.5**- Pore size distributions for the SiO<sub>2</sub> monolith with different concentration of C<sub>18</sub>TAB

**Figure 4.6** - Graph between surfactant concentration and surface area

**Figure 4.7** - the nitrogen adsorption-desorption isotherm for the SiO<sub>2</sub> monoliths with different CTAB surfactant chain length.

**Figure 4.8** - pore size distributions for the SiO<sub>2</sub> monolith with different C<sub>18</sub>TAB chain length.

**Figure 4.9** - SEM Images of C<sub>18</sub>TAB and SDS

## **List of Tables**

**Table 1** - Comparison of the physical and surface properties of a particle column and a monolithic column.

**Table 2** - Effect on the Pore Size and the Pore Volume of Increasing the Amount of PEG (MW 35000 g/mol)<sup>a</sup>.

**Table 3** - Conditions for BET samples.

**Table 4** - Nitrogen physisorption data of samples containing different surfactant.

**Table 5** - Nitrogen physisorption data of samples containing different C<sub>18</sub>TAB surfactant concentration.

**Table 6** - Nitrogen physisorption data of samples containing different C<sub>18</sub>TAB chain length.

## List of Abbreviations and Symbols

❖ °C - degree Celsius
❖ % - Percent
❖ g - grams
❖ mg - milligram
❖ mmol – millimoles
❖ m – meter
❖ cc – centimetre cube
❖ cm - centimeter
❖ M - Molarity
❖ Kg - kilogram
❖ L - litres
❖ min - minutes
❖ nm - nanometre
❖ HPLC - High Performance Liquid Chromatography
❖ Fig - Figure
❖ SEM - Scanning Electron Microscope
❖ PEG – Polyethylene glycol
❖ Conc. - Concentration
❖ BET - Brunauer- Emmett- Teller
❖ CTAB – Cetyltrimethylammoniumbromide
❖ SDS – Sodium Dodecyl Sulphate
❖ TRIX – Triton X-100
❖ BTMAC - Benzyltrimethylammoniumchloride
❖ SiO <sub>2</sub> - Silicon dioxide
❖ Vs. - Versus
❖ STD. – Standard
❖ w.r.t – with respect to

# List of Contents

## Chapter-1

**Introduction.....11-24**

### 1.1. Porous Materials

1.1.1 Microporous Materials

1.1.2 Mesoporous Materials

1.1.3 Macroporous Materials

1.1.4 Applications of Nanoporous Materials in Research and Industry

### 1.2. Monoliths

1.2.1. Overview

1.2.2. Physical Properties of Monoliths

1.2.3. Applications of Monoliths

1.2.4. Advantages of monoliths over particles

1.2.5. Fabrication Methods

### 1.3. Surfactants

1.3.1 Types of surfactants

- Cationic Surfactant
- Anionic Surfactant
- Nonionic Surfactant

### 1.4. Characterization Technique

1.4.1 Nitrogen Sorption Analysis

1.4.2 SEM

## Chapter-2

**2. Literature Review.....25-27**

## Chapter-3

**3. Materials and Methodology.....28-37**

### 3.1. Materials

3.1.1. Apparatus

3.1.2. Reagents and Chemicals used

3.1.3. Surfactants

### 3.2. Instruments Used

3.2.1. Magnetic Stirrer

3.2.2. Weighing Balance

3.2.3. Hot air oven

3.2.4. Muffle Furnace

### 3.3. Methodology

3.3.1. Sol-Gel Processing

- Precursor Materials
- Mixing
- Casting
- Gelation
- Aging
- Drying
- Stabilization
- Calcination

3.3.2. Graphical Representation of Synthesis of Silica Monoliths

## **Chapter-4**

### **4. Results and Discussions.....38-50**

#### 4.1. Morphology

4.1.1. BET Surface Area Analysis and BJH Model

- Effect of Surfactants nature
- Effect of Surfactant Concentration
- Effect of C<sub>18</sub>TAB surfactant chain length

4.1.2. SEM Analysis

## **Chapter-5**

### **Conclusion and Future Prospective.....51**

## **Chapter-6**

### **References.....52-54**

## **1.1 Porous Materials**

A solid material that contains cavities, channels or interstices can be regarded as porous. Nanoporous materials consist of a regular organic or inorganic framework supporting a porous structure. Nanoporous materials are separated into three subtypes: microporous materials, mesoporous materials and macroporous materials. In recent years, nanoporous materials have been recognized as promising candidates for the multifunctional applications such as catalysis are also of scientific and technological importance because of their ability to absorb and cooperate with atoms, ions and molecules on their sizeable interior surfaces and pore space. Nanoporous materials have specifically a high surface to volume ratio, with a high surface area and large porosity, of course, and very ordered, uniform pore structure. A lot of inorganic nanoporous materials are made of oxides. They are often non-toxic, inert, and chemically and thermally stable, although in certain applications the thermal stability requirement is very stringent so you have to have a very highly thermal stable catalyst [1].

### **1.1.1 Microporous Materials**

Microporous materials, such as Metal organic frameworks (MOFs), zeolites, carbons and amorphous glasses, exhibit extremely narrow pore size distributions in the range of 0.5 – 2 nm. These materials can display high thermal stability and catalytic activity useful in cracking processes and can also serve as ion exchange media, drying agents and gas separation materials. Metal organic frameworks (MOFs) are one of the fast growing classes of microporous solids.

### **1.1.2 Mesoporous Materials**

Mesoporous materials are defined as natural or synthetic materials having a pore diameter of 2-50 nm, halfway between the pore sizes that define micro- and macroporous materials. They have a large surface area and are particularly useful for applications in catalysis, separation, and absorption.

### **Why Mesoporous Materials?**

Adsorption is considered to be safest and less expensive remedy to handle this problem than precipitation, ion exchange and membrane filtration. An ideal absorbent is one with uniformly accessible pores, an interlinked pore system, have high surface area, physical and chemical stability.

During the past few years, mesoporous materials have gained a lot of interest as adsorbents for heavy dyes and harmful organic compounds, owing to their ultrahigh surface area, tunable pore diameter and pore surface. They also allow molecular accessibility to large internal

volumes and surface areas [2]. Mesoporous adsorbents have good adsorption capacity and been proved to have great advantages than traditional adsorbents like activated charcoal and resins.

### 1.1.3 Macroporous Materials

In contrast macroporous materials with pores sizes between 50 and 1000 nm such as porous polymer beads allow for easy access to the internal pores at the cost of selectivity. These drawbacks led to the development of mesoporous materials, which have an intermediate pore size range, between 2 – 50 nm.

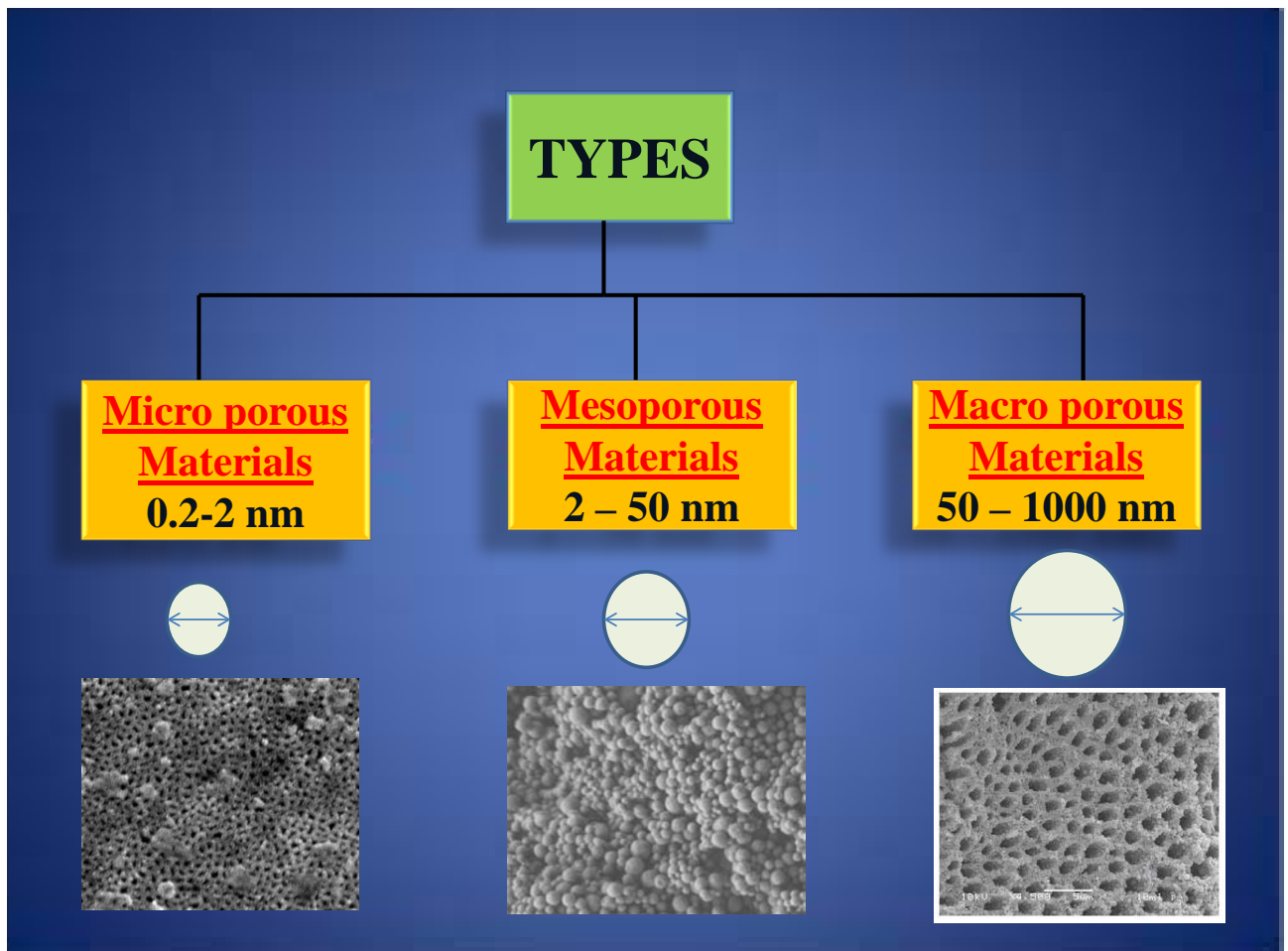


Fig. 1.1 Types of Nanoporous Materials

## **1.1.4 Applications of Porous Materials in Research and Industry**

### **Drug Delivery Systems**

The main challenge in the development of drug delivery systems (DDS) is that drug efficacy diminishes before reaching the target, primarily due to the excretion of the drug from the body. In addition, the drug carrier must be non-toxic and inert during the treatment period. Because most biological molecules and pharmaceuticals are on the order of a few nanometers, nanoporous silica with a pore size of 2 – 30 nm is of great relevance for such life science applications.

### **Catalysis**

In catalysis, high surface area materials with nanoscale features are used to develop highly selective catalysts that reduce energy use and waste/pollutant generation in industrial applications. Porous materials, such as zeolites (microporous solids) are widely used in industry as catalysts and catalyst supports. However, when large molecules are involved in a catalyzed reaction, mass transfer limits the suitability of zeolite structures. Attempts to improve the diffusion of reactants to catalytic sites have been resolved by enlarging pore sizes to the meso range. These ultra-selective catalysts can cut costs significantly in many industries.

### **Diagnostics**

Mesoporous materials are ideal in diagnostics applications due to their increased image contrast and chemical stability. Moreover, functional moieties can be conjugated within the pores enables new possibilities for multiple measurements and detection. Due to the low toxicity of silica based porous materials and their ability to host a variety of fluorescent markers, dyes and drugs can be used to track the location of therapeutic agents and their activity.

### **Adsorbents**

The high surface area of nanoporous materials allows their use as adsorbents for various gases, liquids and toxic heavy metals. The uptake of these substances can be increased significantly based on the surface properties (hydrophobicity, hydrophilicity, or functionality), of the mesoporous silica materials. Several applications, such as removal of pollutants from water, storage of gases (e.g., CO<sub>2</sub>, H<sub>2</sub>, O<sub>2</sub>, CH<sub>4</sub>, H<sub>2</sub>S), adsorptive xylene separation, and separation of biological and pharmaceutical compounds, have been addressed through the use of mesoporous materials as adsorbents.

## Chromatography

The large pore volume, surface area and narrow pore-size distribution of mesoporous silica, makes it a good candidate for size exclusion chromatography. These materials have been proposed as supports or stationary phases for size exclusion chromatography, capillary gas chromatography, proteomics separations, normal phase High Pressure Liquid Chromatography (HPLC), as well as enantioselective HPLC.

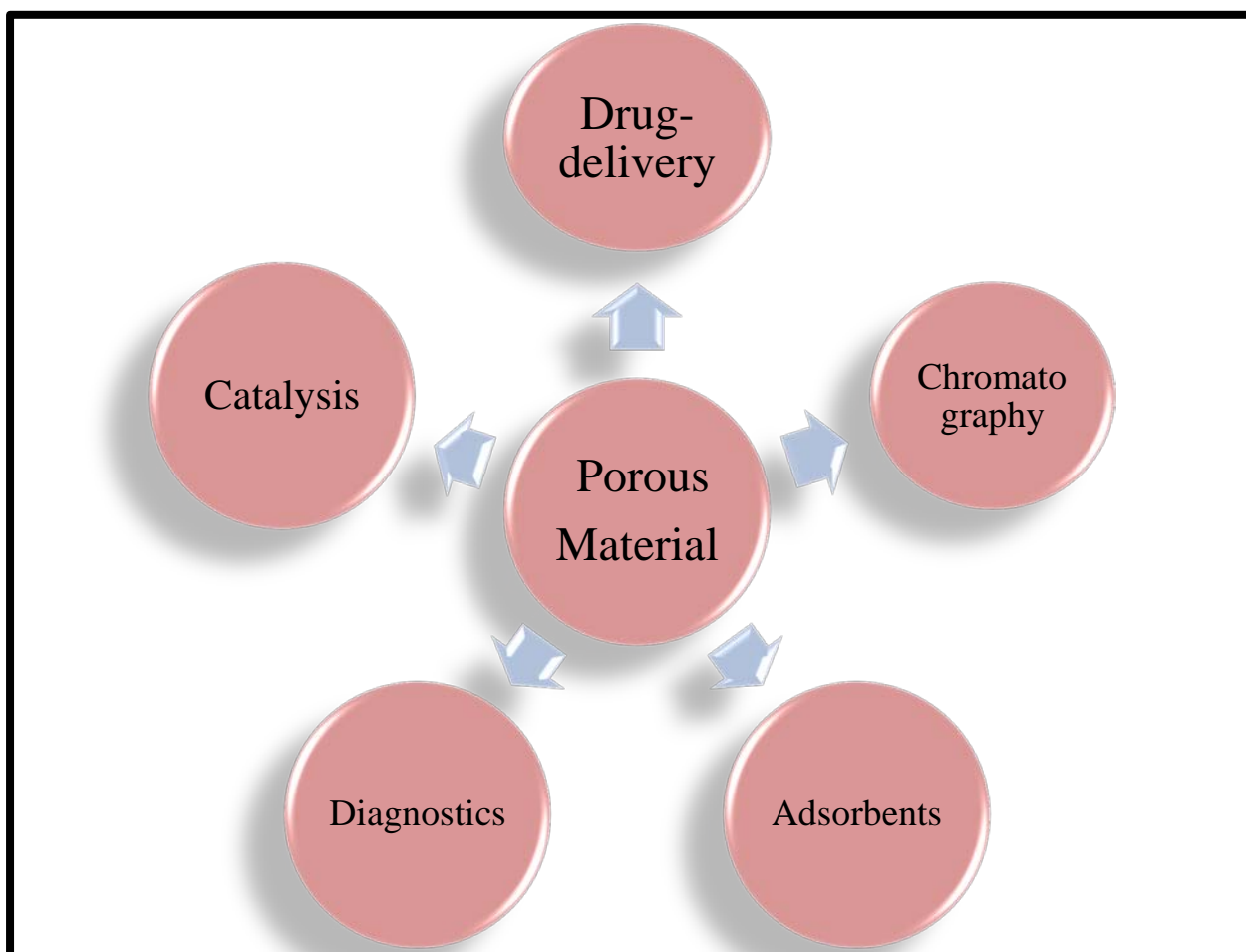


**Fig. 1.2 Application of Nanoporous Materials**

## 1.2 Monoliths

### 1.2.1 Overview

A monolith is a geological feature consisting of a single massive stone or rock, such as some mountains, or a single large piece of rock placed as, or within, a monument or building. Erosion usually exposes the geological formations, which are often made of very hard and solid metamorphic or igneous rock.

According to the IUPAC definition: “A monolith is a shaped, fabricated, intractable article with a homogeneous microstructure that does not exhibit any structural components distinguishable by optical microscopy [3].

In chromatographic terms, monoliths represent a continuous single rod of porous material [Tanaka et al., 2002]. It is characterized by high permeability due to uniform distribution of macropores and mesopores throughout the network enabling separation of many analytes. The macropores present provide the permeability for solvents to flow through, whereas mesopores provide the high surface area for separation. As the formed network fills the column volume completely, interparticulate voids are absent, resulting in 100% flow of mobile phase through the column.

Monoliths are broadly classified on the basis of the nature of materials used for the preparation. Depending on this, there can be many types of monoliths but generally they are categorized into organic and inorganic based monolith. All other types of monoliths revolve around the chemistry of these two types of monoliths, either with certain modifications or by using combination of monomers [4].



**Fig. 1.3 Rock Stone Monolith**

### **1.2.2 Physical Properties of Monoliths**

The properties of silica monoliths are influenced by several factors, including physical parameters, chemical composition and the thermal process that can be used during the fabrication process [5,6]. In general, the structure of silica monoliths contain, large (micron) flow-through pores, with up to 99 % porosity [7], which can give a high permeability and small (Nano) diffusion pores that can generate high surface areas of up to 1,000 m<sup>2</sup> /g [8]. In addition, silica monoliths have good optical transmission (~90 %) [9], low density (~ 50 g cm<sup>-3</sup>) [10], dielectric constant (~ 2) [11] and thermal conductivity (~ 0.05 W/mK) [12].

### **1.2.3 Applications of monoliths**

A number of chemical, catalytic, optical, and thermal applications have been reported based on silica monoliths [13]. In 2006 Randon et al. used inorganic monolithic column for the separation of a mixture of alkoxybenzene (consisting of thiourea, toluene, ethylbenzene, propylbenzene) and amines (consisting of naphthalene, orthotoluidine and aniline) [14]. In 2006 the same group also applied a similar technique for the separation of caffeine, naphthalene, theophylline and 7-( $\beta$ -hydroxyethyl) theophylline in hydrophilic interaction liquid chromatography (HILIC) [15]. The advantage of monolithic shape make it possible to use luminescence therefore, maintaining quantum confinement effects in sol-gel can be achieved by either limiting the dimensionality (density) of the network or by introducing spacers between particles to limit interactions [16,17]. Furthermore, modification of inorganic surface with potassium and platinum made it suitable to be used as catalysts and it shows spurious support properties [18]. In addition, the laser action was also obtained by the interference of multiple scattered light from organic dyes incorporated in the pores of inorganic monoliths [19].

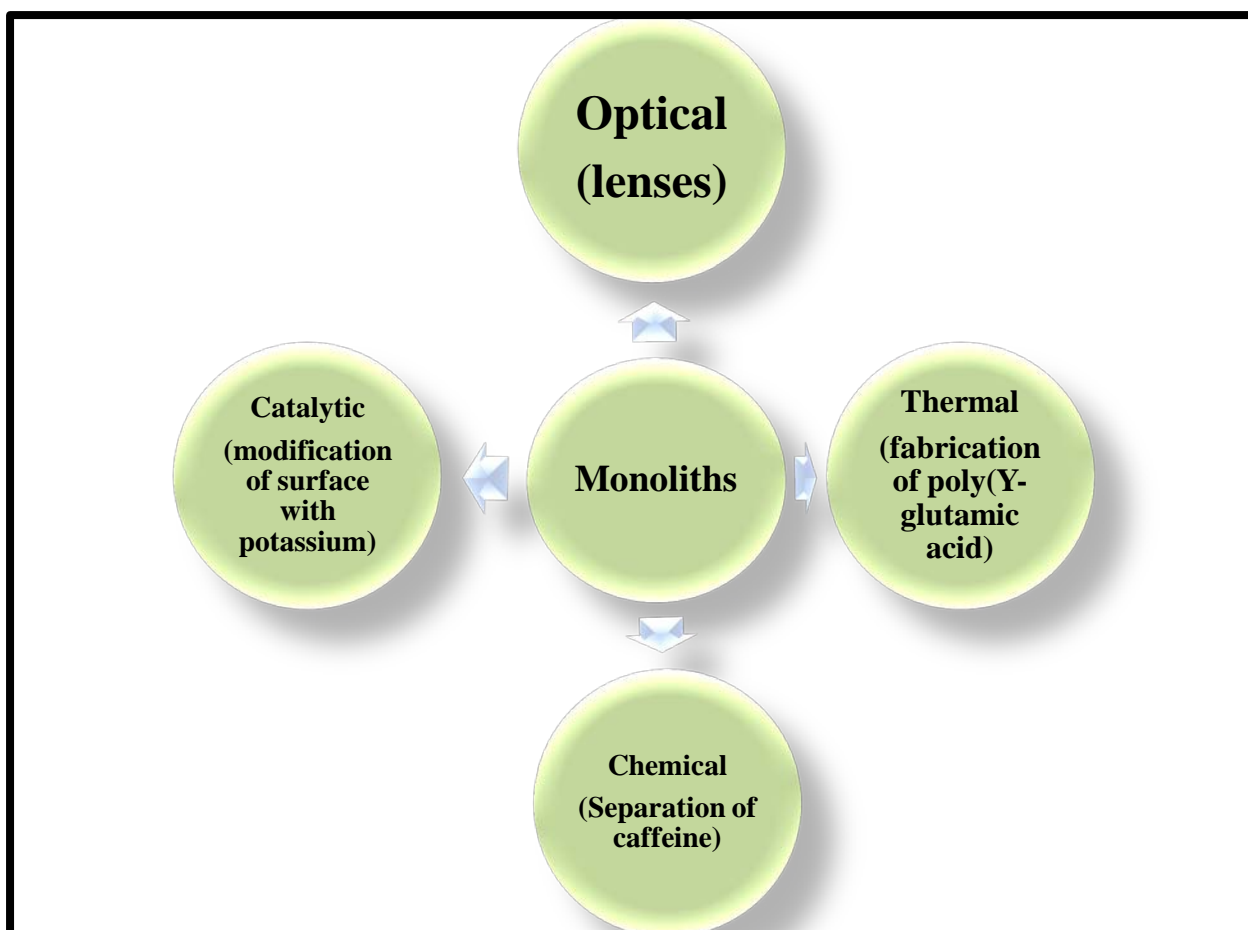


**Fig. 1.4 Application of Monoliths**

### **1.2.4 Advantages of Monoliths over Bulk Particles**

When van Deemter plots of particulate and monolithic columns are compared one major difference is apparent: the contribution of the C term (mass transfer). The C term contribution in monolithic columns is much lower than that of particulate columns [20].

The low value for C with monolithic columns results in a faster partitioning of analytes between the mobile or elution phase and stationary phase, in comparison with particle packed columns. The mass transfer of monolithic columns is usually high. The mass transfer of monolithic stationary phases is attributed to convection rather than diffusion. For that reason the mobile or elution phase in a monolithic column flows through the pores, whereas the majority of the mobile or elution phase, in a packed column, flows between the particles. Other advantages of monolithic stationary phases over particle packed phases include lower back pressures due to their higher permeability, no need frits to retain the phase; ease of modification, and their ability to be produced in different formats (e.g. rod, disks, capillary) [21].

Properties	Monolithic column	Particle packed column
Skeleton size ( $\mu\text{m}$ )	1.3-1.6	-
Particle size ( $\mu\text{m}$ )	-	5
Macropore size ( $\mu\text{m}$ )	2	-
Interparticle pore size ( $\mu\text{m}$ )	-	1.25-2
Mesopore size (A)	130	90
Total porosity	>0.80	0.65
External porosity	0.706	0.37
Surface area ( $\text{m}^2 \text{g}^{-1}$ )	300	340
Total carbon (wt %)	19.5	18

**Table -1 Comparison of the physical and surface properties of a particle column and a monolithic column**

### 1.2.5 Fabrication Methods

The monolithic structures can be defined as rigid macro-porous stationary phases, constructed from either silica or polymer [22]. In the last few decades, the fabrication of macroporous materials has been extensively studied. The formation of the silica network can be achieved by templating close-packed colloidal crystals infiltrated by gas or liquid phase precursors in order to enclose and freeze the structure of the template [23]. Then, removal of the frame can be carried out by either thermal treatment or chemical etching [24]. However, in this case the main drawback of the purely macroporous network is that the low surface areas and a low loading of potential substitution sites for functional groups on the surface [23]. To improve the surface area, new methods for formation of macroporous silica monoliths have been developed. Galarneau and co-workers [25] reported that a pseudomorphic transformation is conducted at the surface of the macroporous, while the size of pores and the particle is preserved. This methodology generated silica materials, which have a high loading of functional organic moieties and a high mechanical stability; however, the surface area was quite low.

Brook and Brennan prepared macroporous silica monoliths based on sol gel process where allyl- and silylmodified poly (ethylene glycol) (PEG) polymers are used to induce aggregation of the particles process and obtained the macroporous network structure. Macroporous materials provide high permeability for large molecules, such as proteins and DNA, however, the high throughput and low specific surface areas, do not make them ideal candidates for extraction of small organic molecules [26,27]. The combination of mesoporous and macroporous in the silica monolithic structure can, however, provide the necessary amount of active sites and high surface areas, in addition to a high diffusion rate for separation, extraction and catalysis applications [28]. A number of approaches towards sponge architecture materials have been developed where the interconnected framework consisting of macropores structure allows for a high solvent diffusion rate and mass transfer, while the

smaller pores (mesoporous) in the skeleton structure increases the surface area and makes the adsorption of small molecules much better [4,29].

In 1992 Nakanishi and co-workers [30] presented one of the most important sol-gel procedures. They prepared a silica-based monolith with bipore structure, combining two processes: phase separation and sol-gel transition. A gel is a state where both solid and liquid are dispersed in each other. The silica monoliths generated were highly porous and offered the potential to be used in different fields of technology, such as electronic, chemical separation, extraction and fabrication, optical, bio-analysis and energy storage [31, 32].



**Fig. 1.5 Monoliths**

## **Synthesis of Porous Materials by Different Surfactants**

### **1.3 Surfactants**

Amphiphilic surface active agents, surfactants, consist of at least two parts; a hydrophilic (head group) and hydrophobic (tail), and they have been widely used as templates for the preparation of mesoporous structures. The tendency to accumulate at an interface (e.g. water-air, water-oil) is a fundamental property of a surfactant. The driving force is the lowering of the interfacial free energy/interfacial tension of the inter phase boundary.

Another fundamental characteristic of surfactants is that the surfactant monomers in a solution tend to form aggregates called micelles. The formation of micelles reduces the free energy of the system since the monomers absorb at the interface by rearranging hydrophobic groups in contact with the water. The formation of micelles depends on the concentration of the surfactant in the solution, and the limit at which the micelles start to form is called the critical micelle concentration (CMC).

Surfactants in a lyotropic system can form different liquid crystal (LC) phases including isotropic micellar, micellar cubic, hexagonal columnar, bicontinuous cubic, lamellar, and reversed micelle phases depending on the concentration and temperature of the system.

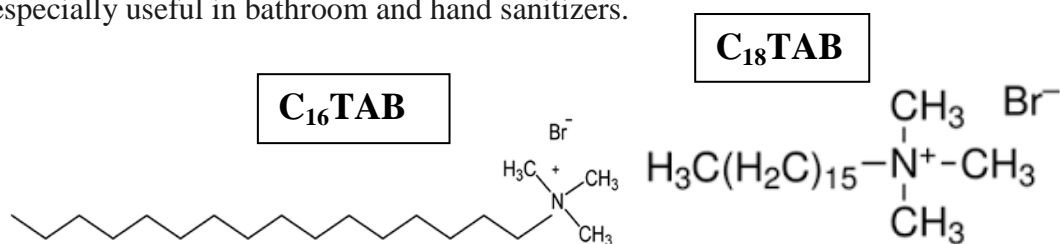
### 1.3.1 Types of Surfactants

Depending on the polarity of the head group, surfactants are classified as anionic, cationic, non-ionic (neutral) and zwitterionic. In addition, a subclass of cationic amphiphilic surfactants called gemini surfactants has attracted much attention with various industrial and academic research groups. These surfactants are more rigid and show special properties such as a low CMC and a high viscosity. A conventional surfactant consists of a linear hydrophobic chain and a polar head group but, a gemini surfactant possesses two hydrophobic and two polar groups which are separated by a spacer's.

Anionic and cationic surfactants with various degrees of head group area and hydrophobic tails of length 12 and 16 respectively were used. The CMC of anionic surfactant is 8.2 mM for SDS at 25°C. The CMC of cationic surfactants is 1.58 mM for cetyltrimethylammonium bromide (C18TMABr) and at 25°C and for non-ionic surfactant Triton X-100 is 0.21 mM at 25°C.

#### 1. Cationic Surfactant

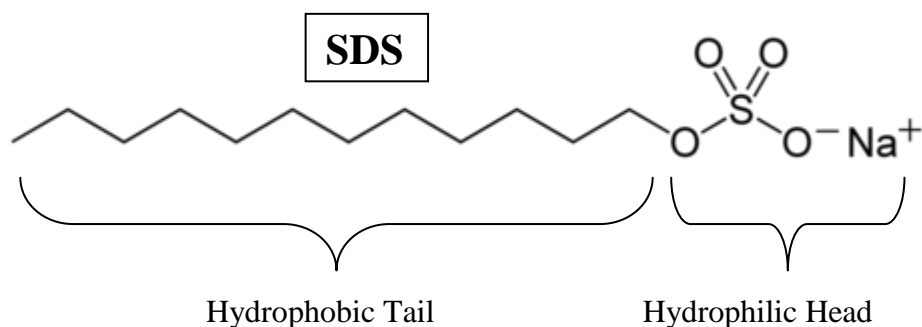
Cationic surfactants are basically soaps or detergents, in which the hydrophilic or water-loving end contains a positively-charged ion or cation. Typical examples are trimethylalkylammonium chlorides and the chlorides or bromides of benzalkonium and alkyipyridinium ions. Cationic surfactants are almost all man-made, and their ionic portion is positively charged. They are good emulsifying agents too, and do not form insoluble scums with positively-charged hard-water ions. These surfactants have also been found to be good bactericides and some find use as topical antiseptics. Their germicidal properties make them especially useful in bathroom and hand sanitizers.



#### 2. Anionic Surfactant

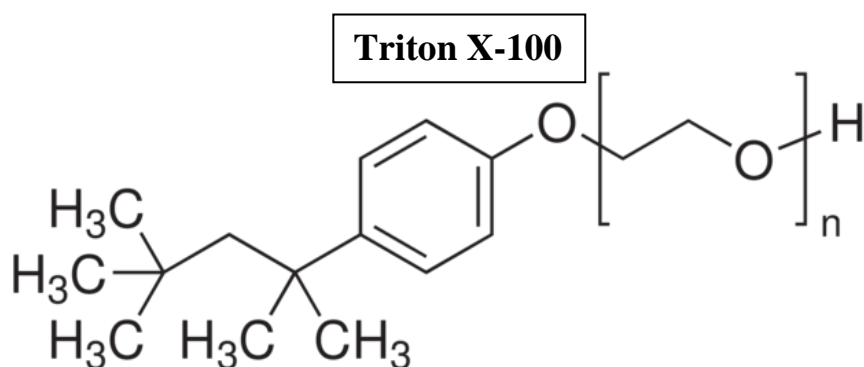
An anionic surfactant is a macromolecule, usually in the sulfonate or sulfate group of chemicals such as sodium laureth sulfate that acts as an active surface agent to lower the surface tension of liquids. This allows them to bind to impurities and particles that are suspended in the liquid, which makes them effective cleaning agents in water. In small concentrations, they can also cause the foaming of compounds in water by creating large

numbers of small bubbles of gas, and this makes them effective in cosmetics such as shampoo, toothpaste, and in fire-suppressing agents.



### 3. Nonionic Surfactant

Nonionic surfactants are a distinct type of surfactant with an uncharged polar head. In horticultural contexts, nonionic surfactants may be known as wetting agents because they help hydrophobic, or water repelling, soils to quickly and evenly absorb water by breaking the water's surface tension, allowing water molecules to spread for greater and faster water penetration.



## 1.4 Characterization Technique

### 1.4.1 Nitrogen Sorption Analysis

One of the characteristic properties of a sol-gel material is its pore structure. Nitrogen adsorption-desorption isotherms data were used in the experiments conducted as part of this dissertation to obtain information about specific surface area and pore structure parameters of the synthesized materials. Isotherms were measured at 77K with a Micromeritics Tristar 3000 automated nitrogen adsorption instrument using the static volumetric determination technique. Before measurement, all samples were degassed by heating at elevated temperature under flowing nitrogen. As shown in Figure 1.6, gas adsorption isotherms have been classified by IUPAC into six different types. Type I is a characteristic adsorption isotherm from microporous solids. Types II, III, and VI are obtained due to adsorption in non-porous or macroporous materials, and Types IV and V arise from adsorption in mesoporous materials. Hysteresis loops appear in Type-IV and V isotherms due to the

irreversible nature of capillary condensation / evaporation, but these types of isotherms can be reversible too (indicated by adsorption and desorption branches that lie on top of each other).

**(a) Specific Surface Area:** Specific surface areas of the finely divided porous materials were evaluated using the standard Brunauer-Emmett-Teller (BET) multilayer adsorption model. The BET method is based on the determination of the monolayer capacity, which is defined as the quantity of adsorbed molecules in a single filled molecular layer on the surface of a material. BET monolayer capacity was calculated by fitting the experimental adsorption data to the linearized form of the BET equation (Equation 2.7) in the range of relative pressures from 0.05 to 0.2:124

$$\frac{x}{v(1-x)} = \frac{1}{v_m c} + \left( \frac{c-1}{v_m c} \right) x \quad (2.7)$$

where  $v$  is the amount of nitrogen adsorbed at any relative pressure  $x$  ( $\equiv p/p_o$ ),  $v_m$  is the monolayer capacity, and  $c$  is a constant related to the heat of adsorption in the first layer. It has been found that the shape of the isotherms in the BET range depends on the numerical value of  $c$ , becoming sharper as the heat of adsorption in the first layer increases. To be consistent while comparing the specific surface areas of different samples, the same relative pressure range was used for all surface area calculations. Monolayer capacity is obtained from the values of slope ( $\equiv \frac{c-1}{v_m c}$ ) and intercept ( $\equiv \frac{1}{v_m c}$ ) of the linear BET plot. The monolayer capacity thus obtained was multiplied by the cross-sectional area of the adsorbed N<sub>2</sub> (assumed to be 0.162 nm based on hexagonal close packing of nitrogen) to estimate the specific surface area of the material [33].

## Types of BET Isotherm Curves

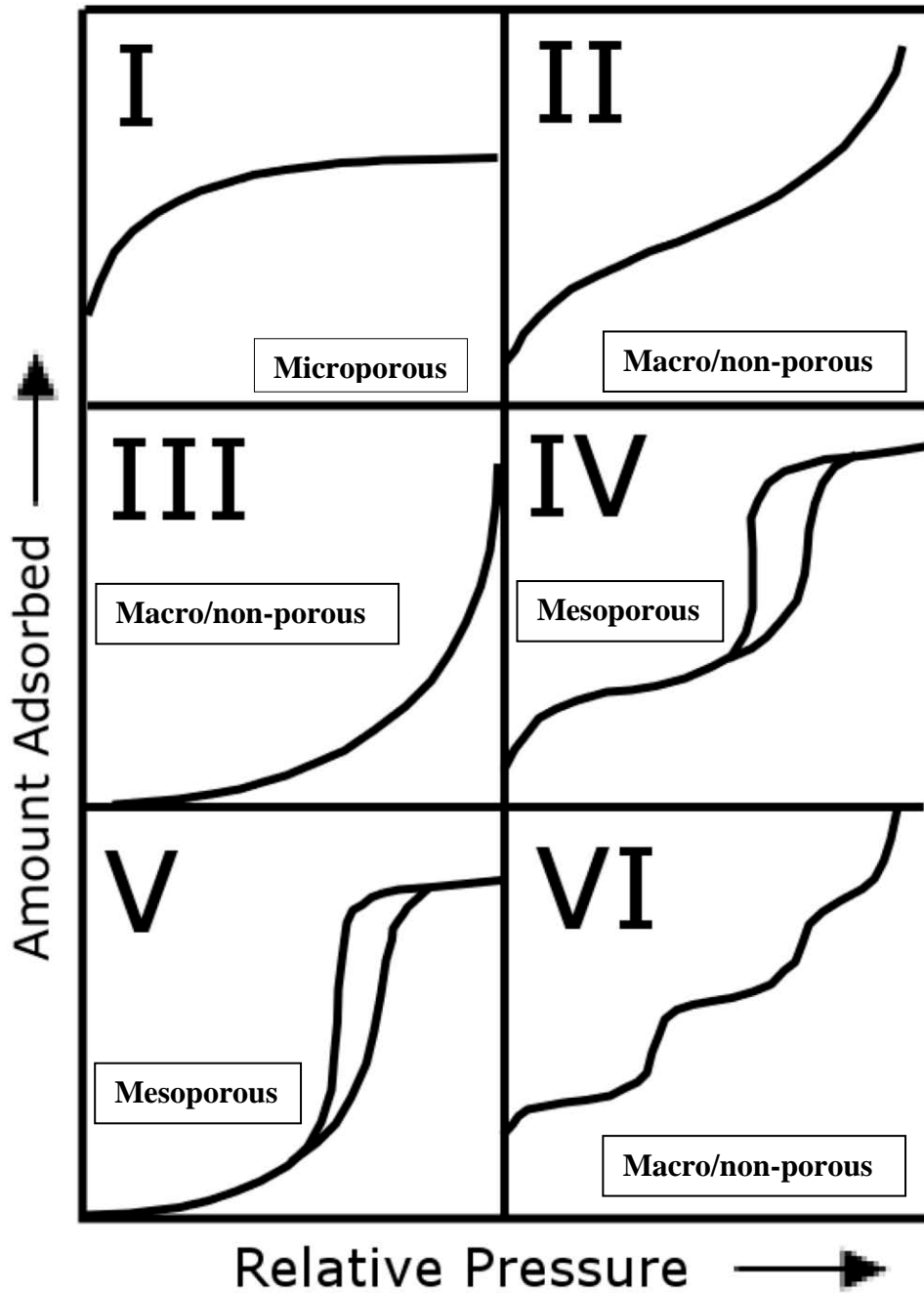


**Fig. 1.6 IUPAC classifications of gas adsorption isotherms (adapted from Sing et.al.5)**



**Fig.1.7 BET Surface Analyzer**

### **1.4.2 SEM (Scanning Electron Microscopy)**

The scanning electron microscope (SEM) uses a focused beam of high-energy electrons to generate a variety of signals at the surface of solid specimens. The signals that derive from electron-sample interactions reveal information about the sample including external morphology (texture), chemical composition, and crystalline structure and orientation of materials making up the sample.



**Fig.1.8 SEM Analyzer**

Monolithic materials have become very popular because of various applications, especially within chromatography and catalysis. Large surface areas and multimodal porosities are great advantages for these applications. New sol-gel preparation methods utilizing phase separation or nanocasting have opened the possibility for preparing materials of silica [3].

The synthesis of porous silica and other oxides has recently attracted immense interest. The use of supra-molecular arrays of surfactants or amphiphilic block copolymers as structure-directing agents for the inorganic framework enables the synthesis of meso-scopically ordered materials exhibiting a narrow pore size distribution after removal of the organic portion. Other recent approaches utilize latex spheres, (micro) emulsion droplets, and macromolecules for the generation of porosity. Furthermore, recent progress in the field of sol-gel chemistry enables macroscopic shape control to be achieved in parallel, and porous oxides have been prepared in the form of films, fibers, and monoliths. This is a necessary step toward expanding the application window of these materials beyond the scope of their use as sorbents, support materials, or the like in the direction of applications in the life science area.

Materials exhibiting micro/macroporosity and meso/macroporosity have been synthesized by the combination of two or more pore building processes, zeolitic nanoparticles, or supramolecularly templated in-organic aggregates in combination with colloidal particles. Gel casting has also successfully been used to create hierarchical zeolitic or mesoporous structures with controlled shapes. Silica spheres have also been successfully transformed into zeolitic monoliths containing interconnected macropores.

Furthermore, mesoporous/macroporous silica has been prepared by coating bacterial threads with silicate-surfactant mesophases. However, chemical means of inducing phase and domain separation during synthesis has also successfully been applied in the synthesis of siliceous materials exhibiting a hierarchical porosity. In a series of papers, Nakanishi and co-workers used a wide variety of water-soluble polymers, such as poly-(ethylene oxide) (PEO), to control the phase separation/ gelation kinetics in the preparation of monolithic silica of virtually any shape exhibiting both interconnected macropores and textural mesoporosity. The macropore diameter can easily be controlled by adjusting the polymer concentration, since the timing of the phase separation relative to the sol-gel transition determines the macropore size. . The walls in this macroporous structure consist of aggregates of silica nanoparticles giving rise to textural mesoporosity in the walls with pore sizes in the 10-20 nm range and a high specific surface area.

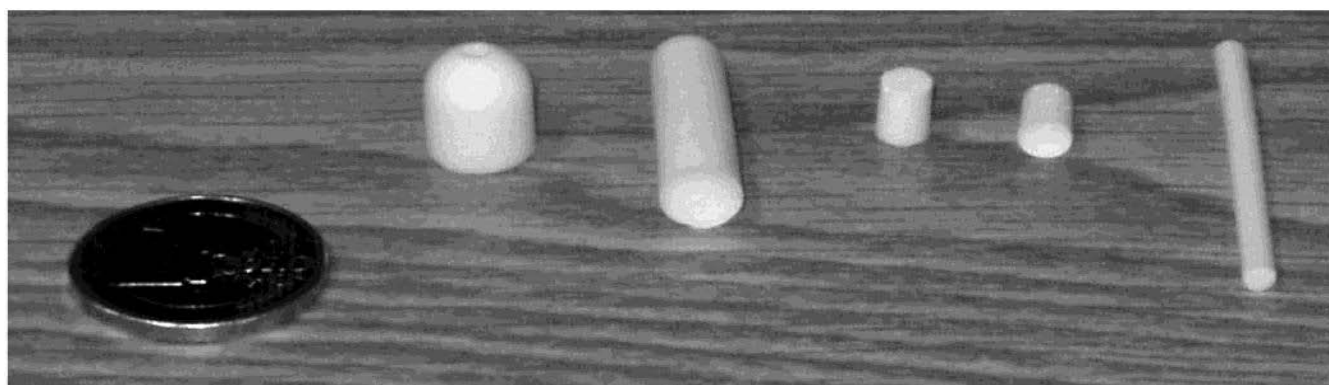


**Fig. 2.1** Photograph of monoliths of different shapes exhibiting multimodal hierarchical porosity. The diameter of the coin is 23 mm.

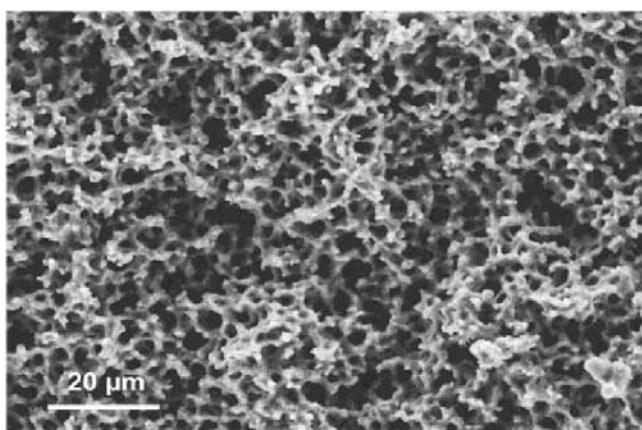


**Fig. 2.2** SEM image of a macroporous sample (Magnification) 1000, scale bar) 20  $\mu\text{m}$ .

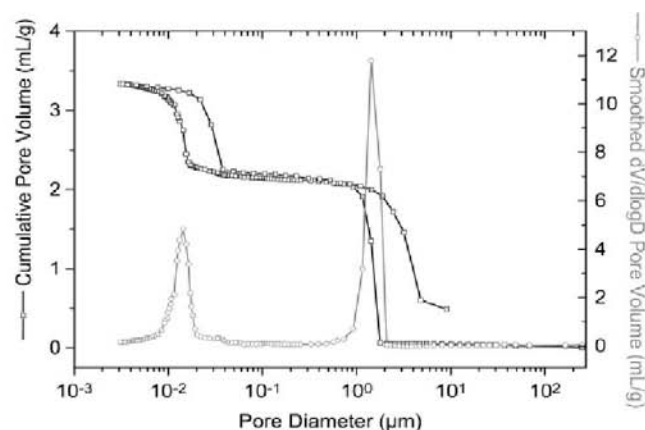


**Fig. 2.3** Pore size distribution of the sample.

sample	PEG/Si	$d_{\text{macro}}^b$ ( $\mu\text{m}$ )	$d_{\text{text}}^b$ (nm)	$V_{\text{macro}}^c$ ( $\text{cm}^3 \text{g}^{-1}$ )	$V_{\text{text}}^d$ ( $\text{cm}^3 \text{g}^{-1}$ )	$V_{\text{tot}}^e$ ( $\text{cm}^3 \text{g}^{-1}$ )
P-54	0.54	12.56	14.4	1.71	1.34	3.06
P-58	0.58	4.24	14.4	1.96	1.04	3.00
P-62	0.62	1.42	14.4	2.17	1.17	3.34
P-65	0.65	0.563	15.6	2.20	1.16	3.36
P-69	0.69	0.263	16.2	2.43	1.02	3.45

**Table – 2** Effect on the Pore Size and the Pore Volume of Increasing the Amount of PEG (MW 35000 g/mol)<sup>a</sup>

where <sup>a</sup> The TEOS/HNO<sub>3</sub>/H<sub>2</sub>O molar ratio was 1.00:0.25:14.69 in all cases. <sup>b</sup> Approximately determined from the mercury intrusion plot. <sup>c</sup> Determined from the cumulative mercury intrusion plot ( $d > 50 \text{ nm}$ ). <sup>d</sup> Determined from the cumulative mercury intrusion plot ( $d < 50 \text{ nm}$ ). <sup>e</sup> Does not contain any nitrogen physisorption contribution ( $V < 0.2 \text{ cm}^3/\text{g}$ ).

Recently, the same group used block copolymers of the  $(EO)_x-(PO)_y-(EO)_x$  type instead of PEO in a similar synthesis, and mono-liths with a similar bimodal pore size distribution could be prepared. In this case, the mesopores were in the 2-3 nm range and were suggested to be structure directed by supramolecular aggregates of the amphiphilic block copolymer, similar to what has been observed for SBA-15 type materials [34].

Stein et al. and later a number of other groups have been using closely packed latex spheres as hard templates for producing three-dimensionally ordered macro-porous materials, while the group of Seshadri has produced macroporous materials from crystalline single-source precursors through decomposition followed by selective leaching of one of the phases. The major drawbacks of these materials are the small window sizes between the cage-like macropores combined with high production costs due to expensive templates in the first system and the limited mesoporosity in the latter. Furthermore, by using anion-exchange resins as macrotemplates a wide variety of inorganic spheres have been prepared, including different zeolite structures. Here, the morphology is restricted to macroscopic beads [35].

However, it is also possible to synthesize highly porous silica using cationic surfactants as structure-directing agents under acidic conditions [34].

The first successful studies on surfactant-organized mesoporous materials were done on the silica system and to date silica remains the most studied material [36].

The motivation for the present work is to try to combine two synthesis approaches in the synthesis of monolithic silica exhibiting multimodal porosity, the first one being polymer-controlled phase separation of silica particles during gelation in combination with a second approach using surfactants that can act as a supra-molecular template [34].

Thus in this thesis the second approach using different types of surfactants for phase separation of silica particles during gelation is shown.

Our work aims to study the effect of different types of surfactant, their variation in the concentration and chain length on the textural parameters (such as pore size and pore volume) and on the enhancement of surface area.

This chapter deals with the materials and methodology used during research work which includes chemicals, glass wares, instrument like Brunauer–Emmett–Teller (BET). SEM was used to characterize the silica monoliths.

### **3.1 Materials**

#### **3.1.1 Apparatus**

Beakers (50ml and 250 ml), micro pipette, measuring cylinder, filter paper, glass rod, magnetic beads, reagent bottles, Petri plates, Elisa plate, tips, falcon tubes, spatula, crucible and magnetic stirrer for the preparation solution.

#### **3.1.2 Reagents and Chemicals Used**

Tetraethoxysilane (TEOS) was purchased from Alfa Aser. C<sub>16</sub>TAB was purchased from Himedia. Poly (ethylene glycol) PEG with (MW 35 000 g/mol) was purchased from Sigma Aldrich. BTMAC, Triton X-100 and C<sub>14</sub>TAB were purchased from Loba Chemie and C<sub>18</sub>TAB obtained from TCI. C<sub>10</sub>TAB and C<sub>12</sub>TAB were obtained from spectrochem. Nitric acid (69%) was used as the catalyst for the hydrolysis and condensation of TEOS. Ammonia (28-30%) was used in post-treatments of the monoliths and SDS was purchased from Merck, miliQ water.

#### **3.1.3 Surfactant**

Cetyltrimethylammoniumbromide [(C<sub>18</sub>H<sub>33</sub>)N(CH<sub>3</sub>)<sub>3</sub>Br;CTAB] is a quaternary ammonium surfactant. It is one of the components of the topical antiseptic cetrimide. The cetrimonium (hexadecyltrimethylammonium) cation is an effective antiseptic agent against bacteria and fungi. It is also one of the main components of the buffer for the extraction of DNA. It has been widely used in synthesis of gold nanoparticles (*e.g.*, spheres, rods, bipyramids), mesoporous silica nanoparticles (*e.g.*, MCM-41), and hair conditioning products. Due to its relatively high cost, is typically only used in select cosmetics.

As with most surfactants, CTAB forms micelles in aqueous solutions. At 303 K (30°C) it forms micelles with aggregation number 75-120 (depending on method of determination; average ~95) and degree of ionization,  $\alpha = 0.2-0.1$  (fractional charge; from low to high concentration).

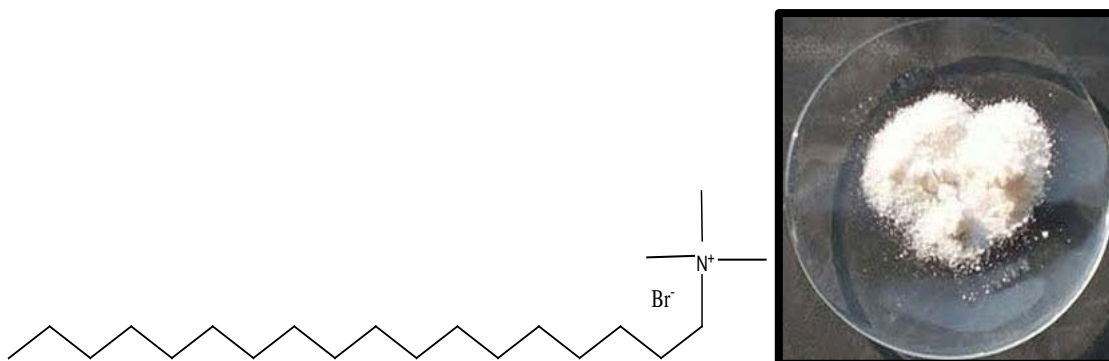


**Fig. 3.1 Structure of Trimethylstearylammoniumbromide (C<sub>18</sub>TAB)**

### 3.2 Instrument Used

#### 3.2.1 Magnetic Stirrer

A magnetic stirrer of REMI 2MLH is a laboratory device which uses magnetic field to mix liquid samples, since only a small magnetic bar has to put inside the liquid sample to start the process of mixing. It is used in the experiment for mixing surfactant with TEOS and PEG into the solution. Magnetic stirrer often includes a hot plate or some other means for heating the liquid.

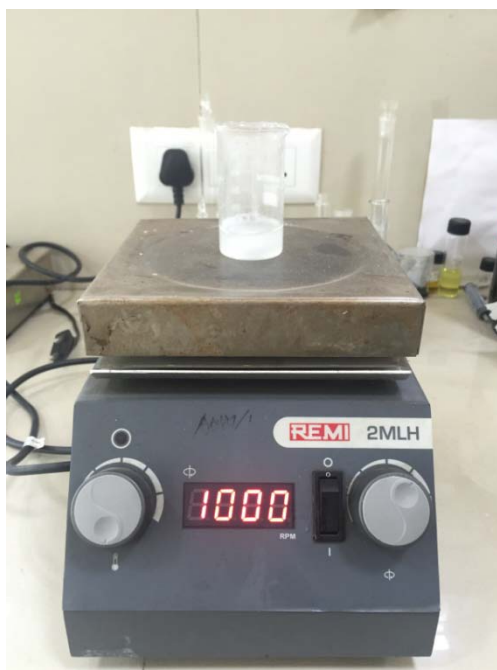


**Fig. 3.2 Synthesis of Surfactant Solution on Magnetic Stirrer**

### 3.2.2 Weighing Balance

Accurate quantities of used chemicals can be achieved with the help of weighing balance (SARTORIUS) Maximum-250 gm; Denisty-0.01 mg.



**Fig. 3.3 Sartorius Weighing Balance**

### 3.2.3 Hot Air Oven

The hot air oven also known as digital temp indicator cum controller of PHYSILAB was used to gel the surfactant solution and also to obtain large textural pores monoliths in a 1 M  $\text{NH}_4\text{OH}$  solution. Generally they are operated at the temperature of  $40^\circ\text{C}$  &  $80^\circ\text{C}$  respectively using a thermostat to control the temperature.



**Fig. 3.4 Hot Air Oven**

### 3.2.4 Muffle Furnace

A muffle furnace (PREFIT INDIA) is box type oven for high temperature applications. These are used in various research labs by chemists in order to determine the proportion of sample which is non-combustible and non-volatile. It is used to calcine the samples. Calcination is a thermal treatment process for the removal of volatile fraction. Muffle furnace consists of externally heated chamber, so that material being heated has no contact with the flame. The muffle furnace can achieve a maximum temperature of 1000 °C.



**Fig. 3.5 Muffle Furnace**

## Methodology

### 3.3.1 Sol-Gel Processing

As noted above, the low temperature used for sol-gel processing enables the incorporation of organic surfactant or imprint molecules into the silica network. The sol-gel process is a convenient route to pure, homogeneous silica materials and the structural properties of the fabricated materials, such as mean pore size, pore size distribution, and pore interconnectivity, can be tuned using the process parameters described below. Because of its influence on the structure of silica gels, the mechanism of the sol-gel silica formation process is discussed here, as well as the effects of process parameters on the properties of the final material [33].

The general sequence of steps involved in the sol-gel process is shown in (Fig. 3.6).

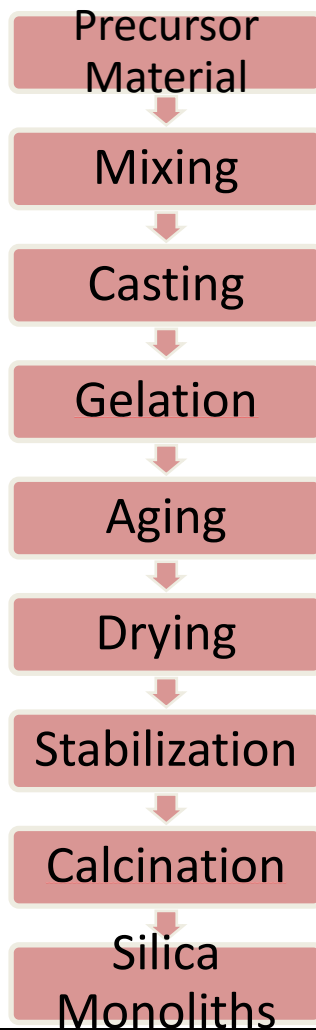


**Fig. 3.6 General Steps Involved In The Production Of Silica Monolith.**

### **STEP 1 - Precursor Materials**

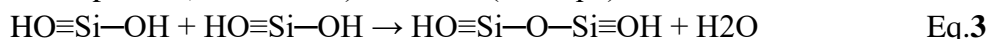
Different types of precursors can be used to form a silica monolithic structure. The most common precursors used in the sol-gel process are metal alkoxides (such as tetraethylorthosilicate/TEOS). These precursors have an organic group attached to a negatively charged oxygen linked to a metal atom [33].

### **STEP II - Mixing**

In this step a liquid alkoxide is hydrolyzed with water to form a homogeneous solution. The hydrolysis reaction using TEOS is illustrated in Eq.2. The TEOS is a type of metal alkoxide used in this research.



The hydrolysis reaction resulted in the formation of silicon hydroxyl groups. The interaction of these silicon hydroxyl groups (Si-OH) with each other is known as condensation and this produces siloxane species ( $\equiv\text{O}-\text{Si}-\text{O}\equiv$ ) and  $\text{H}_2\text{O}$  (see Eq.3).



The condensation reaction continues and a three-dimensional network is formed according to polycondensation behavior [37].

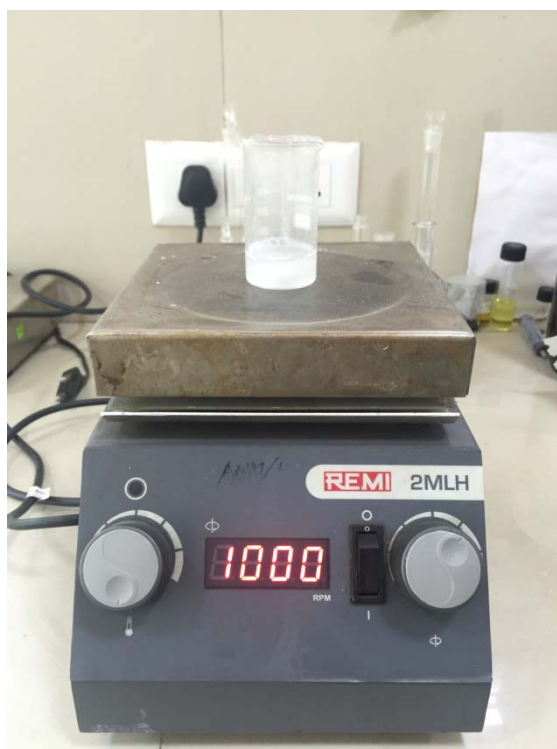


**Fig. 3.7 Mixing**

### **STEP III - Casting**

The casting process consists of pouring a partially polymerized solution into a mould before its viscosity becomes too high. The casting process can be influenced by several factors such as:

1. The shape of the container that can determine the shape of the final product.
2. The quality of the surface of the container that can affect the surface of the product.
3. The type of the mould to eliminate any reaction between the mould and solution.
4. Cleanliness of the container to prevent any contamination.

In the current work the gelation plates is used as mould for the fabrication of silica monoliths.

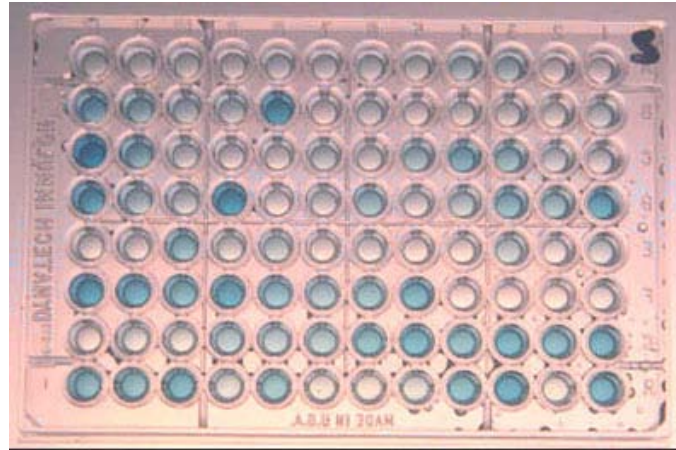


**Fig. 3.8 Casting Process**

#### **STEP IV - Gelation**

In sol-gel processing, a gel will form from the sol after hydrolysis and condensation proceed for a certain period of time. Gelation happens as clusters of condensed silica species or colloidal particles grow through condensation into a network. Eventually a cluster of particles links together into a sample-spanning three-dimensional network, called the gel. At the gelation point, the viscosity of the sol increases sharply and the gel (a liquid-filled porous solid object) takes the shape of the vessel. The network formed has a large enough elastic modulus that it can support a small stress, for example by tilting the vessel, without flowing. The sudden increase in viscosity with a loss of fluidity indicates the gel point, so the gelation time can be approximated (at least as a lower estimate) as the time at which the fluid loses its fluidity. While the gel point signals a dramatic change in connectivity of the network in the sample, hydrolysis and condensation are not complete, and they continue after the gelation point so that during aging, short chain polymers adhere to the gel.<sup>96</sup>This strengthens the gel, but also can create internal stress which causes a gel to shrink and react through a process called syneresis. In this way, the properties of the gel continue to evolve for a significant time after gelation [33].



**Fig. 3.9 Gelation of Monolith**

## **STEP V - Aging**

In the aging step the structure of the gel can be changed according to pH, solvent, temperature and time of aging process. Flexibility in the formation of the gel, make it more viscous and condense, which releases the liquid from the interior phase and shrinkage of the wet gel structure.

There are three possible explanations for this contraction:

- i. Increased bridging bonds due to continuing condensation reactions.
- ii. Dissolution and reprecipitation of the silica primary particulates on the surface of the network structure.
- iii. Addition of new monomers or linkage of un-reacted oligomers after the gelation process.

During the aging process the thickness and strength of the skeleton structure increased and porosity of the monolith decreased.

## **STEP VI - Drying**

During the drying process, solvent and the reaction byproducts (water and alcohol) evaporate from the pores of the gel. Initially the volume shrinkage of the gel is equal to the volume of liquid evaporated and at this point an air-liquid interface exists at the exterior surface of the gel body. Loss of liquid from the interior of the gel creates tensile stress in the liquid and compressive stress on solid. At this stage the bulk modulus of the gel determines the extent of its shrinkage. As drying proceeds, the solid network becomes increasingly stiff because of ongoing localized condensation. When the body becomes too stiff to shrink, the network stops shrinking and further capillary evaporation causes liquid menisci to recede into the pores. Once the pores are empty, the compressive stress on the gel is released. However, if condensation reactions occurred while the gel was compressed, tensile stress develops. Because gels are more resistant to compressive stress than tensile stress, the dried gel may crack unless they are dried very slowly or under conditions that reduce surface tension (such as supercritical drying). Most gels prepared under acidic conditions break apart during drying, while gels prepared under basic conditions may retain their integrity because of both greater network strength and less shrinkage during drying [33].

## **STEP VII - Stabilization**

There are a huge number of silanol groups (SOH) on the surface area of the monolithic structure. An increase in the number of OH groups on the internal surface of the silica monoliths can reduce their transparency. Furthermore, these free negative groups can cause an interaction with the analytes group during the separation and extraction processes. Removing the OH groups from the internal surface of the silica monolith requires a thermal or chemical treatment to take place.

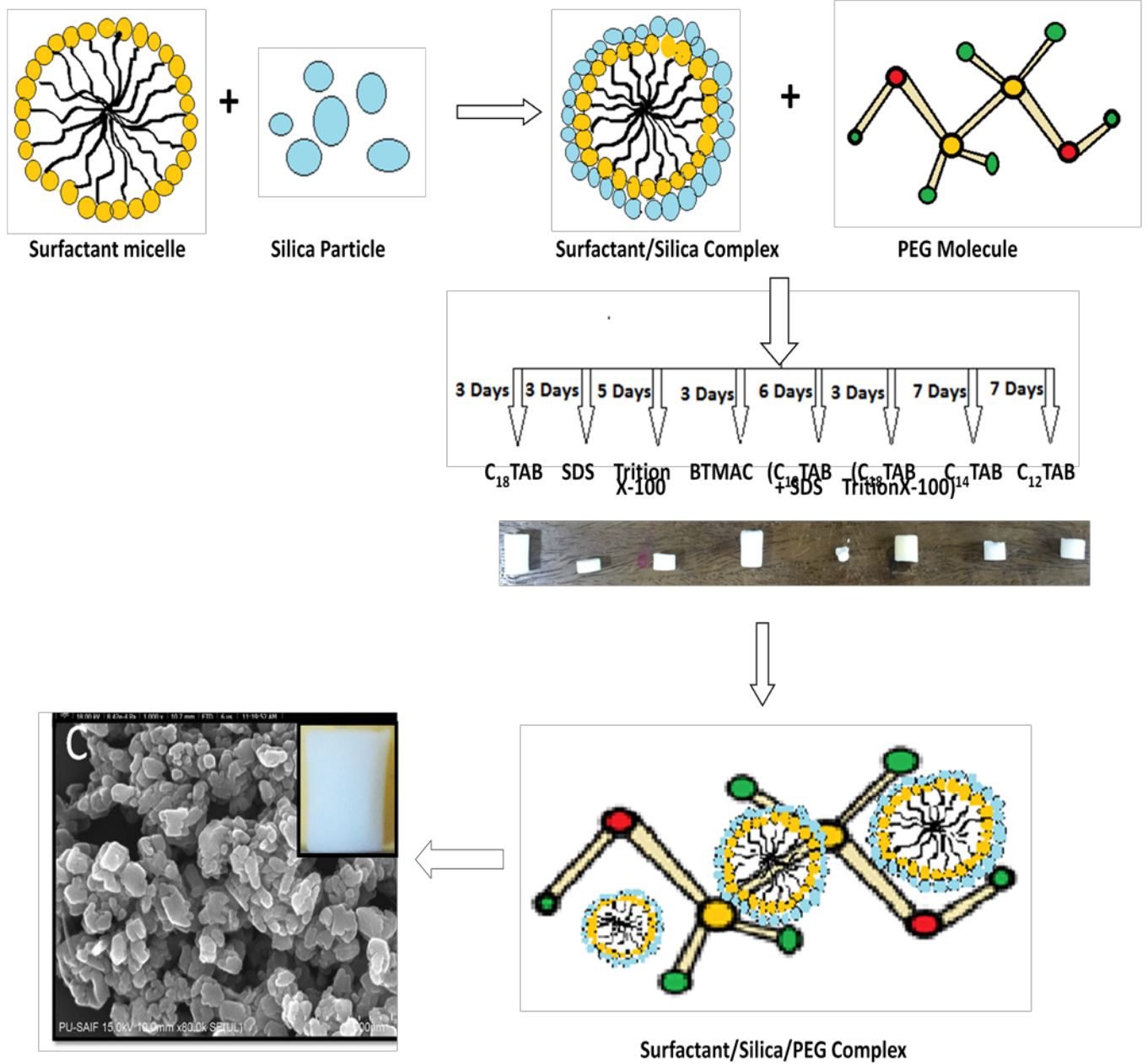
## STEP VIII - Calcination

After drying and stabilization of the silica monolith, subsequent heat treatment is carried out to decompose the organic residues without serious deformation on the monolithic structure [38].



**Fig. 3.10 Different Monoliths Formed By Sol-Gel Process.**

## Graphical Representation of Synthesis of Silica Monoliths



## Chapter-4                      Results and Discussions

Based upon the composition of various samples and content of surfactant loaded in mesoporous silica samples were characterized with the help of different techniques and the respective results were discussed as follows.

### 4.1 Morphology

#### 4.1.1 BET Surface Area Analysis and BJH Model

The physical properties of silica monoliths such as surface area, mesoporous size and mesoporous volume can be measured through a physisorption technique. In the physisorption method, the nitrogen gas adsorb in the silica monolith structure at constant temperature. The amount of adsorbed gas in a sol-gel material depends on the applied pressure [38].

Physical adsorption results from relatively weak Vander Waals forces between the adsorbate gas molecules and adsorbent surface area of test powder [39] .

This determination is usually carried out at the temperature of liquid nitrogen. The amount of gas adsorbed can be measured by a volumetric or continuous flow procedure. The data is treated according to BET adsorption isotherm equation.

$$\frac{x}{v(1-x)} = \frac{1}{v_m c} + \left( \frac{c-1}{v_m c} \right) x$$

$x = P/P_0$

$P$  = Partial vapor pressure of adsorbate gas in equilibrium with the surface at 77.4 k, in Pascals.

$P_0$  = saturated pressure of adsorbate gas.

$V$  = volume of gas adsorbed at standard temperature and pressure.

$V_m$  = volume of gas adsorbed at STP to produce an apparent monolayer on the sample surface.

$C$  = dimensionless constant which is related to the enthalpy of adsorption.

For, single point measurement the specific surface area of monolith from a single value of  $V$  measured at a single value of  $P/P_0$  using the equation given below for calculating  $V_m$ :

$$S = \frac{V_m N \alpha}{m * 22400}$$

Then,  $V_m$  is calculated from single value of  $V$  which is measured at a single value of  $P/P_0$  by the below equation:

$$V_m = V \alpha \left( 1 - \frac{P}{P_0} \right)$$

The error associated with single point measurements is very less as compared to multi point measurements.

In this study BET single point measurement analysis was done for different surfactant nano composites and the experimental conditions are given in Table-3.

Ambient Temp	N <sub>2</sub> % in Cylinder	Regeneration Temperature	Regeneration Time	Sample Dry Wt.	Injected N <sub>2</sub> vol.	Sample Loss (%)
25 °C	70%	150 °C	60 min	23.39g	5cc	0.00%

**Table -3 Conditions for BET Samples**

### 1. Effect of Surfactants Nature :

To check the effect of nature of surfactants on the pore size as well as surface area of monoliths, we have prepared silica monoliths by using cationic, anionic, neutral as well as mixture of cationic-anionic and cationic-neutral surfactants. In this case we have used SDS as anionic, BTMAC, (CTAB) as cationic and Triton-X 100 (TRIX) as non-ionic surfactant. The batches had a general molar composition of H<sub>2</sub>O/HNO<sub>3</sub>/TEOS/ PEG (35, 000)/surfactant molar ratio of these monoliths was 8.2:0.53:2.2:9.54×10<sup>-4</sup>:0.2, in which either a single surfactant or an equimolar mixture of surfactants was present. Figure 4.1 shows the nitrogen adsorption-desorption isotherm for the SiO<sub>2</sub> monoliths with different surfactants. Amorphous structures were produced from the anionic surfactants sodiumdodecyl sulfate (SDS), while the cationic surfactant Cetyltrimethylammonium bromide (CTAB) developed lamellar mesoporous structures with various degrees of crystallinity. Whereas the non-ionic surfactant Triton X-100 fabricated high-quality ordered and hydrothermally stable mesoporous solids [40].

It has been observed that the BET surface area for cationic surfactant, C<sub>18</sub>TAB is 782.54 m<sup>2</sup>g<sup>-1</sup>, while the pore volume and pore diameter are 1.26cm<sup>3</sup>g<sup>-1</sup> and 6.4 nm respectively. But for the anionic surfactant, SDS the BET surface area and pore volume decreased to 210.21m<sup>2</sup>g<sup>-1</sup> and 1.013cm<sup>3</sup>g<sup>-1</sup> while its mesopore diameter increased to 19.31 nm w.r.t C<sub>18</sub>TAB. The surface area for another cationic surfactant, BTMAC is more than the anionic surfactant having value of 441.74 m<sup>2</sup>g<sup>-1</sup> while its pore volume and pore diameter are less. For non-ionic surfactant (TRIX), the surface area 227.05 m<sup>2</sup>g<sup>-1</sup> is in between that of cationic and anionic surfactant i.e. is less than the cationic surfactant but more than the anionic surfactant. For cationic-anionic mixture (C<sub>18</sub>TAB + SDS) the surface is high 295.30 m<sup>2</sup>g<sup>-1</sup> than for the cationic-non-ionic mixture (C<sub>18</sub>TAB + TRIX) having low surface area, i.e. 256.78 m<sup>2</sup>g<sup>-1</sup>. The BET surface area analyses is summarized in the Table-4.

Sample	Nature of Surfactant	BET surface area [m <sup>2</sup> /g]	Pore volume [cm <sup>3</sup> /g]	Pore diameter [nm]
CTAB	Cationic	782.54	1.26	6.4
BTMAC	Cationic	441.74	1.09	9.93
SDS	Anionic	210.21	1.01	19.31
TRIX	Non-ionic	227.05	1.24	21.89
CTAB + SDS	Cationic-anionic	295.30	0.432	5.86
CTAB +TRIX	Cationic-nonionic	256.78	1.46	22.74

**Table – 4 Nitrogen Physisorption Data of Samples containing Different Surfactant**

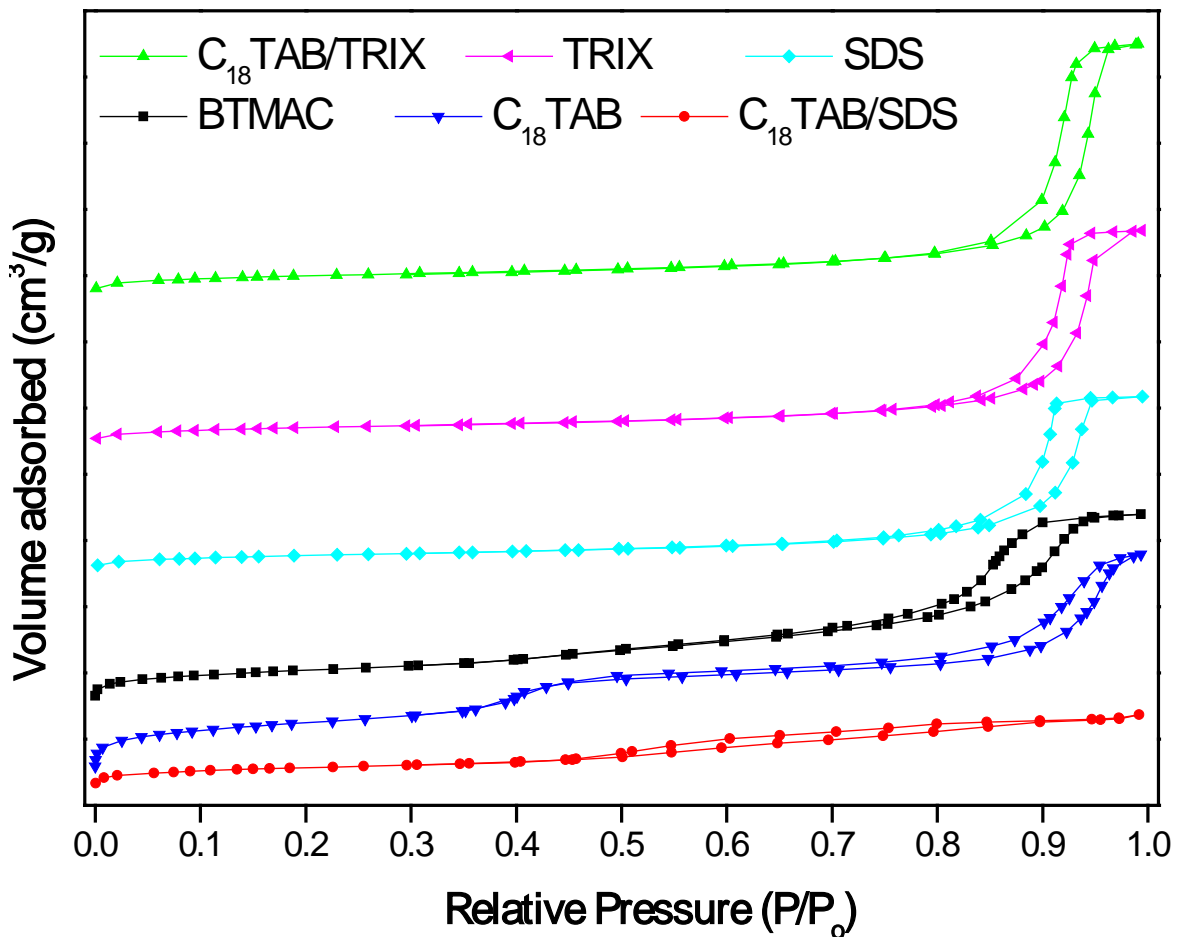


**Fig. 4.1 The nitrogen adsorption-desorption isotherm for the SiO<sub>2</sub> monoliths with different surfactant.**

This result could be attributed to the fact that the critical micelle concentration (CMC) of CTAB in aqueous solution was 0.9–1 mM<sup>48</sup>. Above the CMC, a transition from spherical micelles to rod-like micelles occurred. So on addition of CTAB it forms positively charged rod-like micelles which will insist to make a template of large mesoporous size. Also, there is strong electrostatic attraction between CTAB and TEOS and as a result its pore size increases leading to higher surface area as compared to other surfactants. In case of anionic surfactant SDS it forms negatively charged micelles with small mesoporous size. Thus on addition of TEOS which is also negatively charged results into strong forces of electrostatic repulsions causing lesser interactions among it and leads to decrease in pore size as well as surface area in comparison with the cationic surfactant CTAB. For the nonionic surfactant, the electrostatic force (attractive as well as repulsive) is minimum which leads to form average surface area of monoliths. But in the case of mixtures where the cationic-anionic micelle forms strong electrostatic attraction with TEOS resulting into high surface area whereas the cationic-nonionic mixture micelle results into weak electrostatic attraction with TEOS showing less interactions thereby having lower surface area.

The pore size distribution of various surfactants is shown in Fig 4.2.

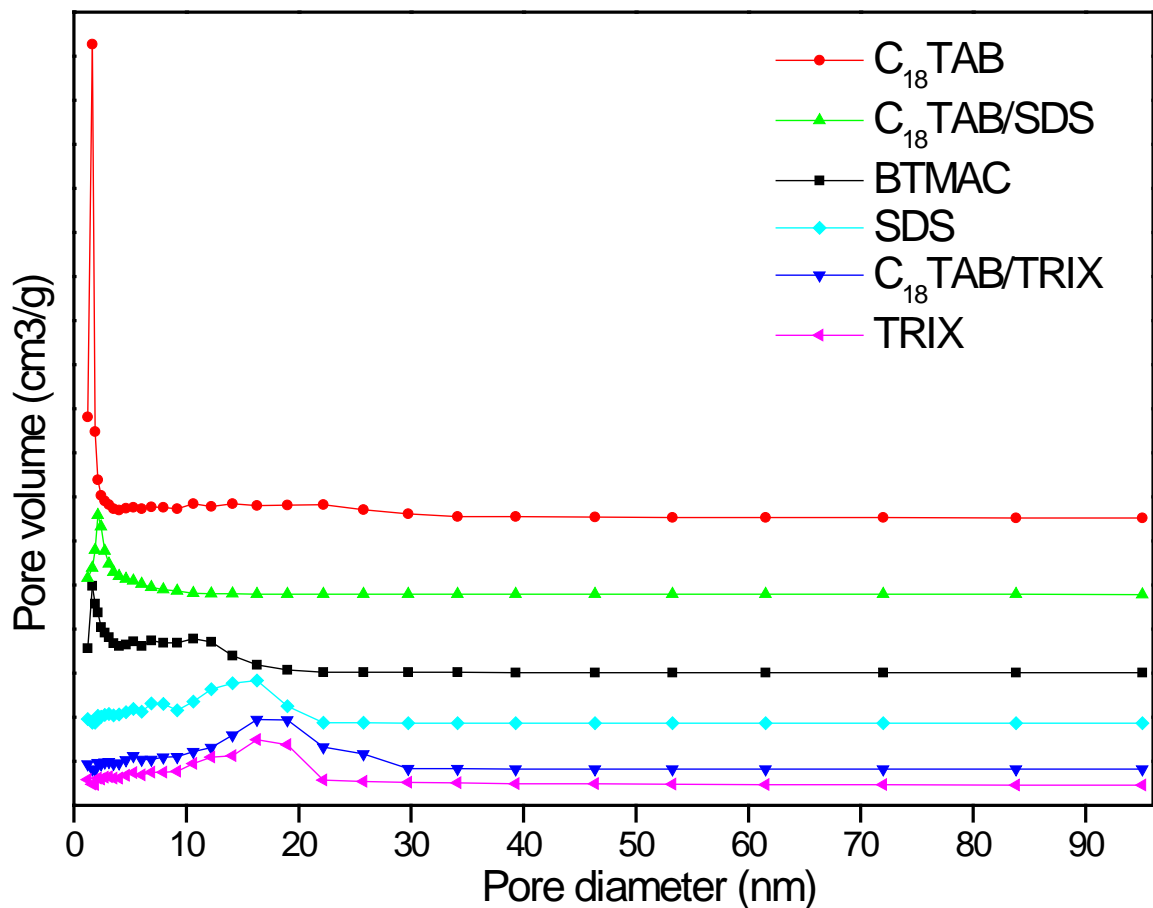


**Fig. 4.2 Pore size distributions for the SiO<sub>2</sub> monolith with different surfactants.**

## Plot of Type of surfactant V/s Surface Area

The Type of surfactant plays an important role in shaping textural parameters (pore size, pore volume) and enhancement of surface area. This graph clearly shows that the cationic surfactant shows the maximum surface area as compared with the anionic, non-ionic and mixture surfactants. This is mainly due to the large attractive forces between the cationic micelle and the precursor (Fig.4.3).

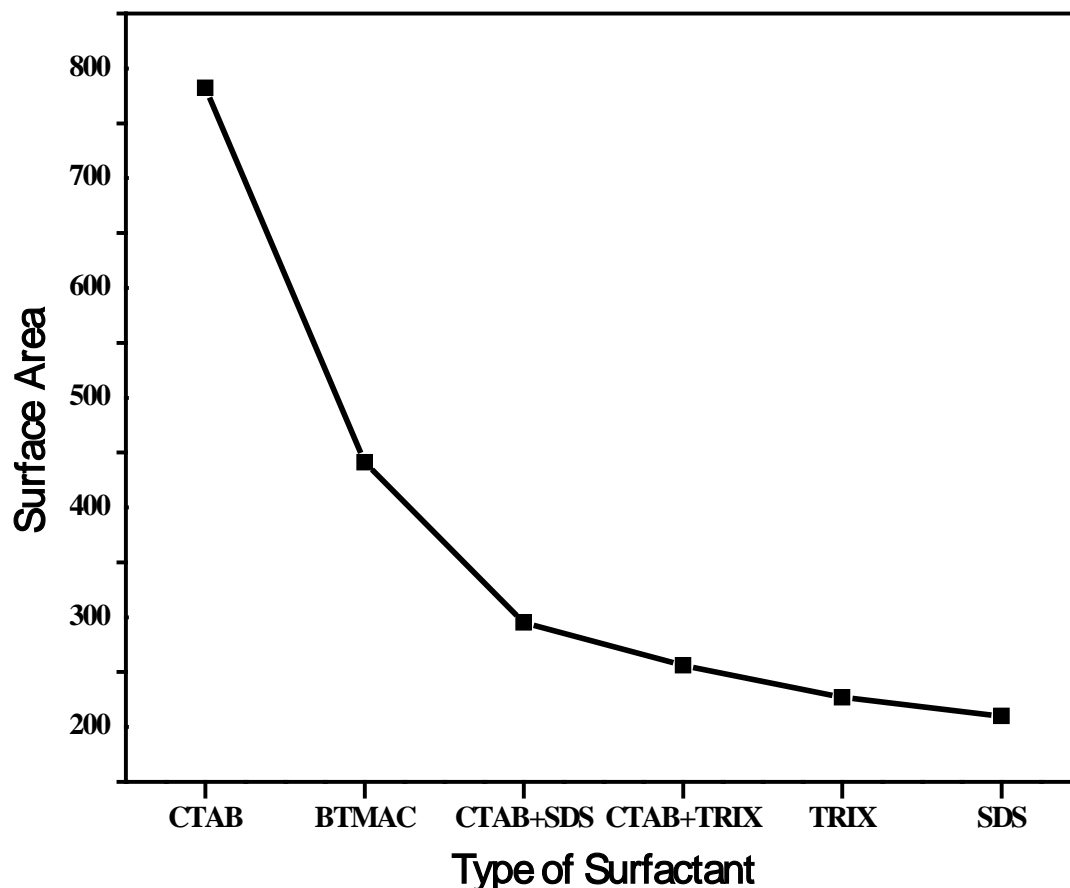


**Fig. 4.3 Graph between type of surfactant and surface area.**

### **2. Effect of Surfactant Concentration:**

Concentration of surfactant strongly influences the textural and morphological properties of mesoporous monoliths. It was observed that the mesopore size increases with the molar concentration of CTAB. This could be attributed to fact that at 40°C temperature, the cations of CTAB aggregated into mixed micelles with TEOS-precursors and acted as templates for the mesopore of silica monoliths. The sample with 0.1mmol of C<sub>18</sub>TAB surfactant had a BET surface area of around 316.33 m<sup>2</sup>g<sup>-1</sup> while the sample with 0.2mmol of C<sub>18</sub>TAB surfactant had a BET surface area of around 782.54 m<sup>2</sup>g<sup>-1</sup> whereas that of sample with 0.3mmol of C<sub>18</sub>TAB surfactant had a BET surface area of around 831.24m<sup>2</sup>g<sup>-1</sup> while sample with 0.5mmol of C<sub>18</sub>TAB surfactant have surface area of 994.52 m<sup>2</sup>g<sup>-1</sup> (Table-5 &

Fig.4.4). Thus there is a direct proportional relationship between the specific surface area and the concentration of the surfactant used in the synthesis of monoliths. This is due to the reason that above the CMC, a transition from spherical micelles to rod-like micelles occurred. So on addition of higher concentrated CTAB, it forms positively charged rod-like micelles which will insist to make a template of large mesoporous size (Figure 4.5). Also, as the concentration of CTAB is increased there is strong electrostatic attraction with the TEOS and as a result its pore size increases leading to higher surface area.

<b>C<sub>18</sub>TAB Concentration [ mM]</b>	<b>BET surface area [m<sup>2</sup>/g]</b>	<b>mesopore volume [cm<sup>3</sup>/g]</b>	<b>mesopore diameter [nm]</b>
0.1	316.33	1.23	15.61
0.2	782.54	1.26	6.40
0.3	831.24	1.09	5.28
0.5	994.52	1.77	7.12

**Table- 5 Nitrogen physisorption data of samples containing different C<sub>18</sub>TAB surfactant concentration.**

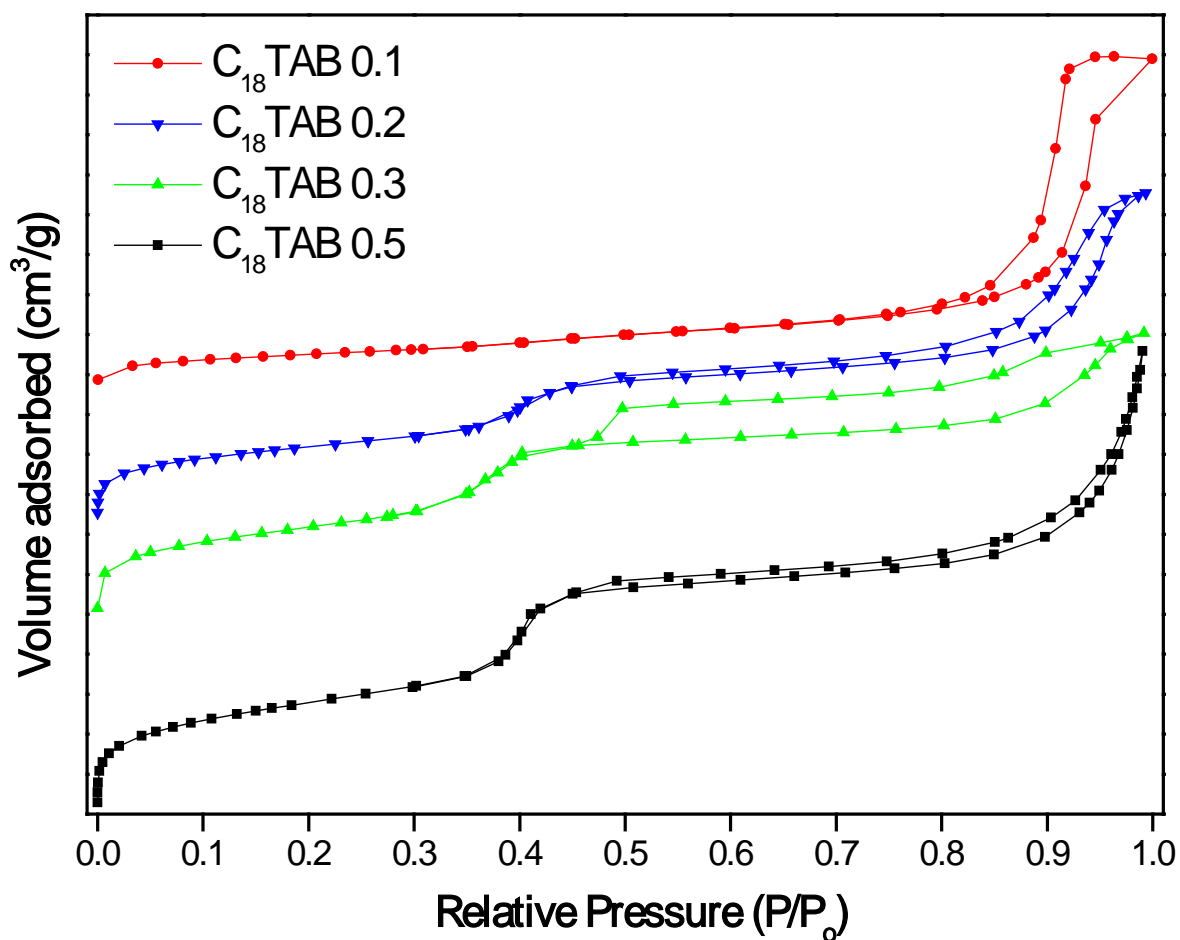


**Fig. 4.4** The nitrogen adsorption-desorption isotherm for the SiO<sub>2</sub> monoliths with different C<sub>18</sub>TAB surfactant concentration.

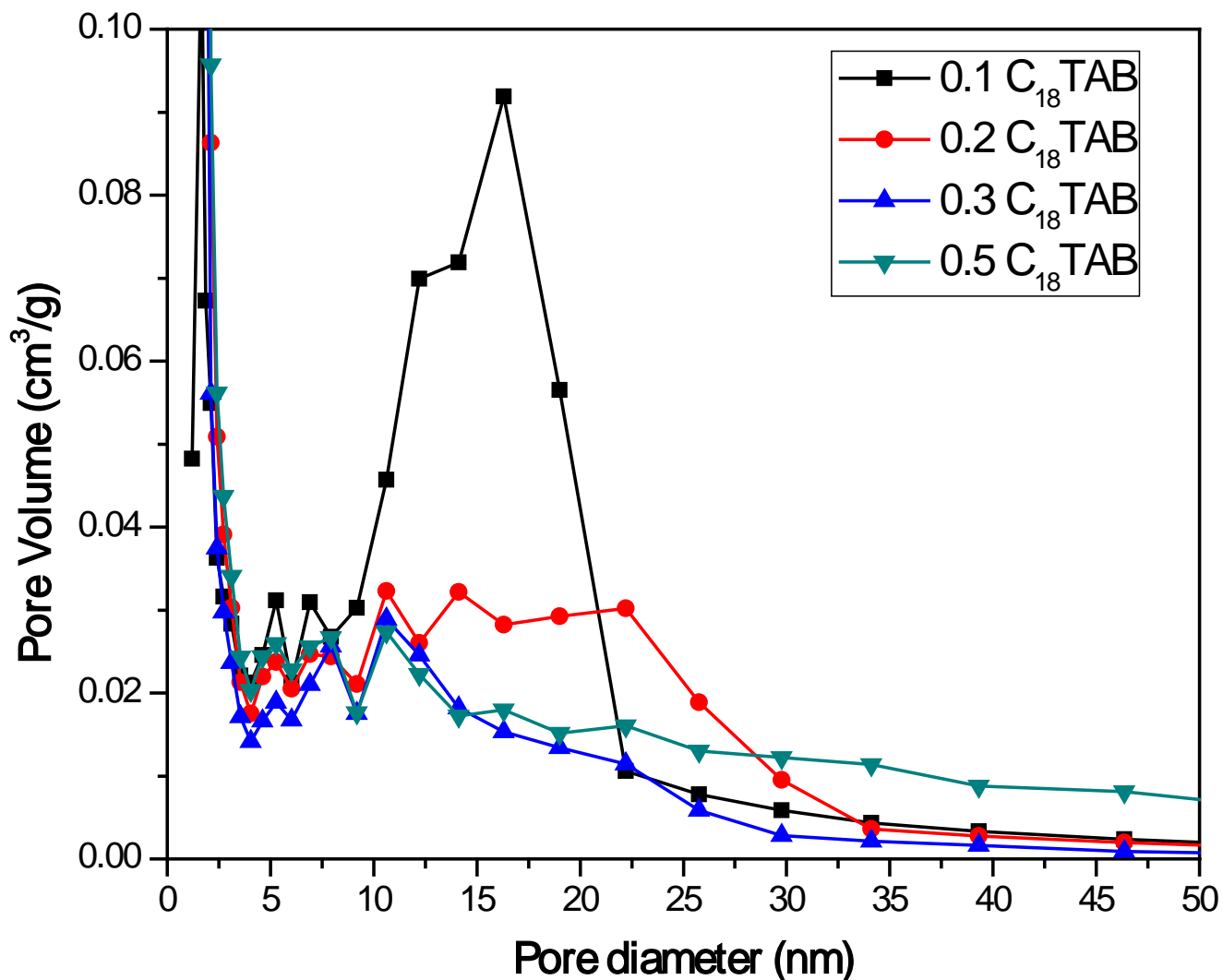


**Fig. 4.5 Pore size distributions for the SiO<sub>2</sub> monolith with different concentration of C<sub>18</sub>TAB**

**Plot of Surfactant V/s Concentration**

The above plot between the type of surfactant and surface area showed that the cationic surfactant results into maximum surface area. So on a similar pattern by varying the concentration of the cationic surfactant it is observed that the surface area increases with the concentration. This is due the reason that on addition of higher concentrated CTAB, it forms positively charged rod-like micelles which will insist to make a template of large mesoporous size and results into higher surface area monoliths (Fig.4.6).

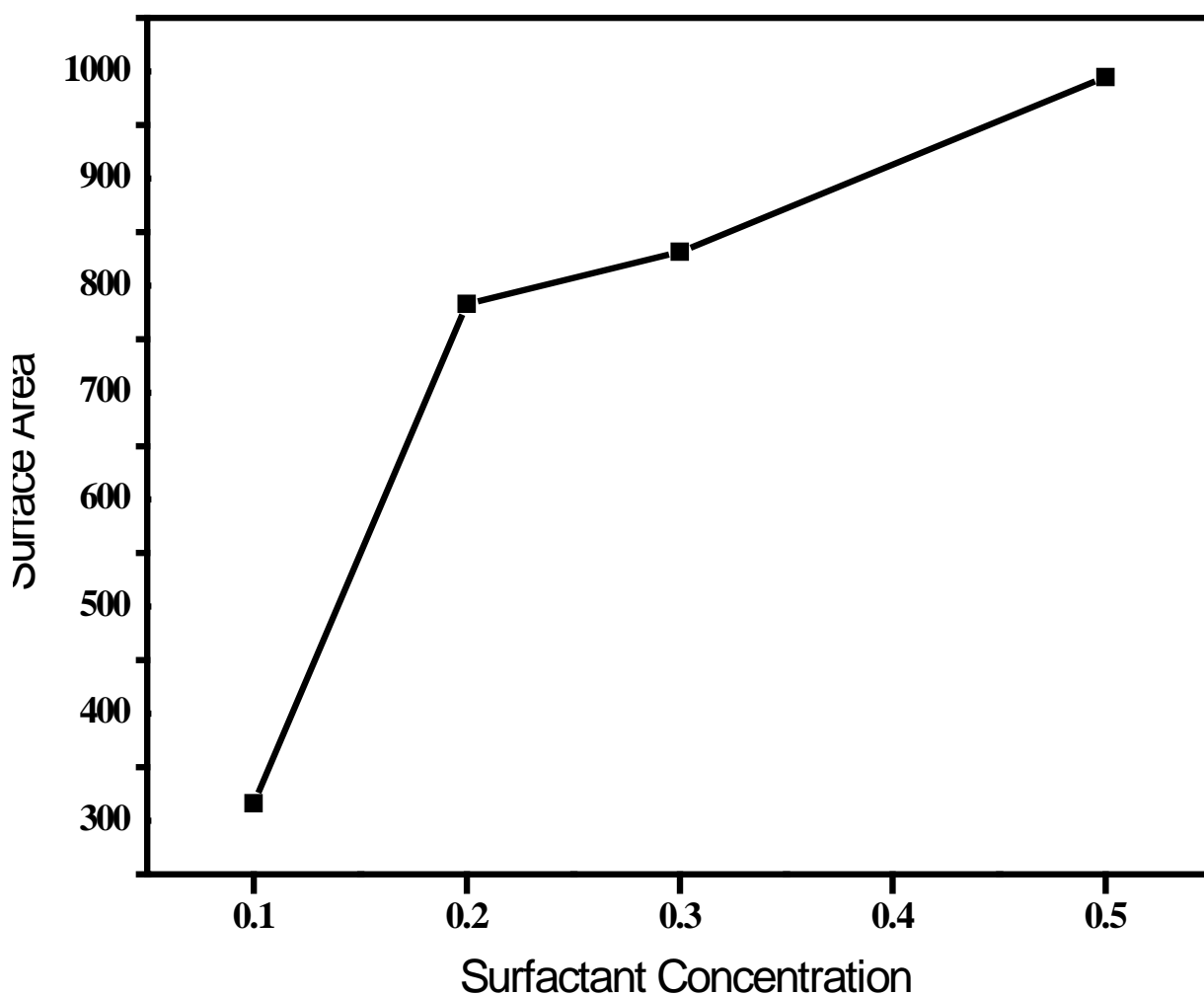


**Fig. 4.6 Graph between surfactant concentration and surface area**

### **3. Effect of C<sub>18</sub>TAB Surfactant Chain Length:**

Some signs of the mesopores can be obtained from the characterization of samples prepared at constant PEG/TEOS and C<sub>n</sub>TAB/TEOS ratios but with surfactant of different chain lengths (n=12, 14, 18). It is clearly seen that the relative pressure at which a markable increase in the adsorption is observed, is shifted to higher values with increasing surfactant chain length Fig 4.7. A dramatic effect of the surfactant chain length is the decrease in the mesopore size with increasing surfactant chain length, as reported in Table 6 and Fig 4.8.

<b>Sample</b>	<b>BET surface area [m<sup>2</sup>/g]</b>	<b>mesopore volume [cm<sup>3</sup>/g]</b>	<b>Mesopore diameter [nm]</b>
C <sub>12</sub> TAB	528.64	1.34	10.15
C <sub>14</sub> TAB	498.08	1.25	10.04
C <sub>18</sub> TAB	782.54	1.26	6.40

**Table -6 Nitrogen physisorption data of samples containing different C<sub>18</sub>TAB chain length.**

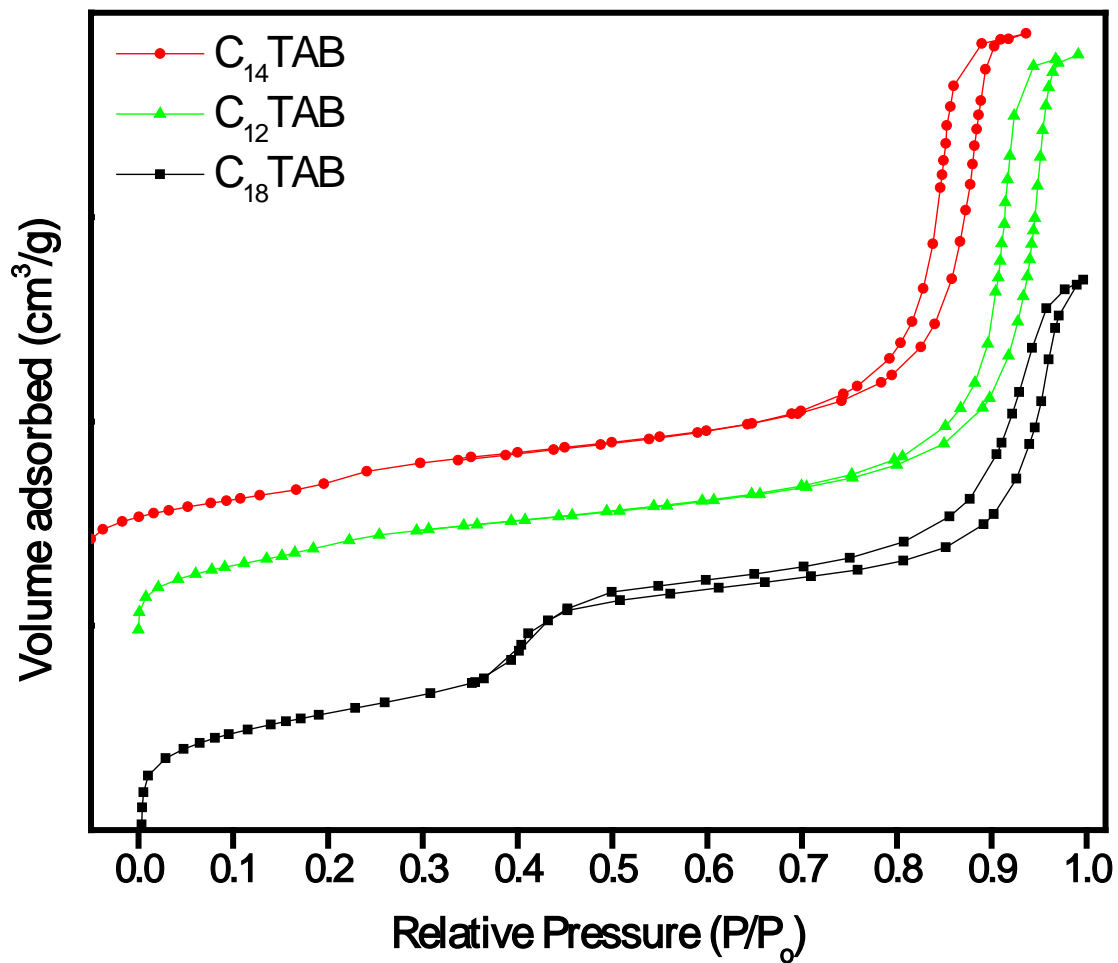


**Fig. 4.7** The nitrogen adsorption-desorption isotherm for the SiO<sub>2</sub> monoliths with different CTAB surfactant chain length.

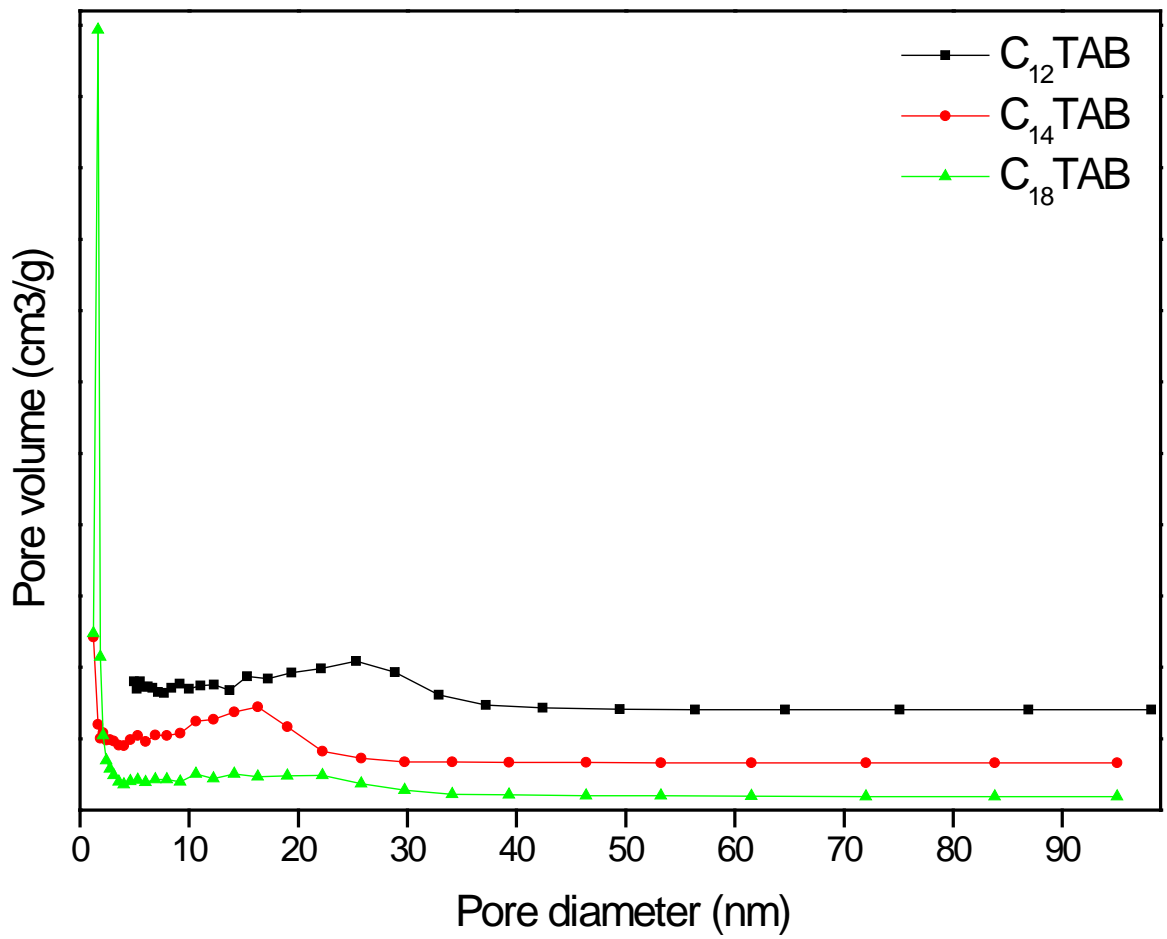


**Fig. 4.8 Pore size distributions for the SiO<sub>2</sub> monolith with different C<sub>18</sub>TAB chain length.**

### 4.1.2 SEM Analysis

One of the most important methods for the analysis of modified stationary phase is scanning electron microscopy (SEM). SEM analysis allows investigating the morphological structure of silica monoliths, which can image each single point within the silica surface at the micrometre down to the nanometre level [38].

The Figure exhibited well defined mesopore (Fig 4.9). The spectra clearly indicate the presence of only two elements which are silicon and surfactant and absence of other elements in the structure.

The characterization results showed that the prepared silica monolith had the characteristics that made it suitable for various applications [4].

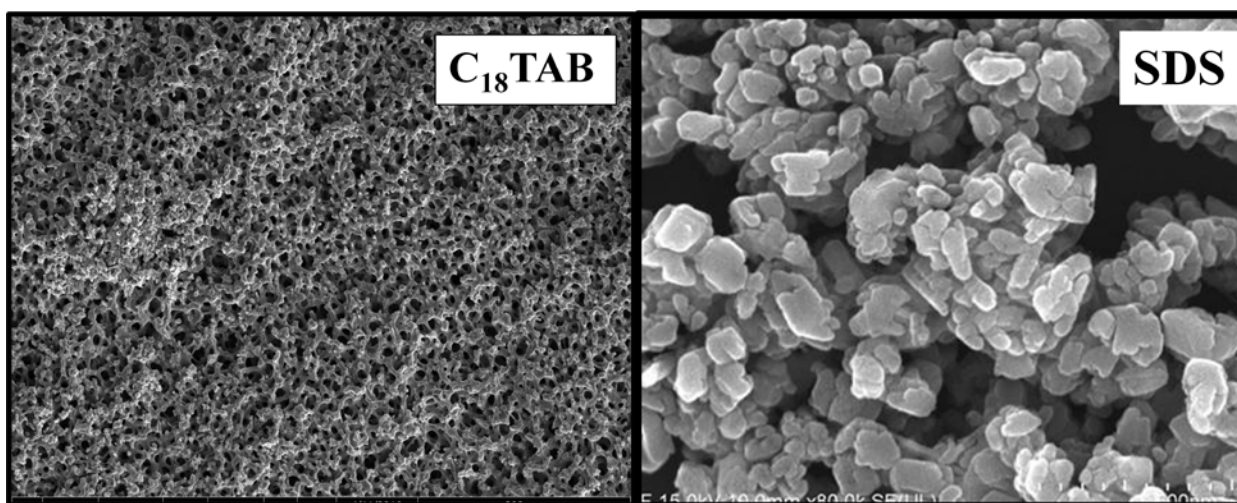


**Fig.4.9 SEM Images of C<sub>18</sub>TAB and SDS**

In conclusion we have fabricated a silica monolith templated with surfactant. Monoliths are example of mesoporous silica supports and are characterized by long parallel channels separated by thin walls. Sol-gel-process is successfully used to prepare monolithic silica having a trimodal, stratified pore structure.

A combination of instruments was used to characterize the property and activity of silica monolith like SEM and BET surface area.

The experiment results indicate that the incorporation of surfactant into the silica monolith could enhance the activity of materials. The particular composition of silica nanoporous material having greater surfactant concentration is more important due to the high surface area. This is due to reason of existing higher forces of attraction between the micelle and the surfactant. The high stability of the silica monolith has lot of applications in several industries.

This work provides method to fabricate silica monoliths templated with different types of surfactant having high surface area and more adsorptivity than the earlier methods.

### **Future Prospective**

- ❖ To Study the porosity of material w.r.t variation in types of surfactants.
- ❖ To Study the porosity of material w.r.t variation in concentration of surfactant.
- ❖ To Study the porosity of material w.r.t variation in the chain length of surfactant.
- ❖ To fabricate trimodal, stratified pore structured monoliths.

1. Lu, G. Q. "Nanoporous materials—an overview." Nanoporous materials: science and engineering 4 (2004).
2. Pagliaro, M., John Wiley & Sons, "Nano-age: how nanotechnology changes our future2011".
3. Bartłomiej Gawęł, Kamila Gawęł and Gisle Øye\* Ugelstad Laboratory, Department of Chemical Engineering, Norwegian University of Science and Technology (NTNU)
4. Nema T, Chan ECY, Ho PC. "Application of silica-based monolith as solid phase extraction cartridge for extracting polar compounds from urine". Talanta 2010. 82:488-494.
5. H. Minakuchi, K. Nakanishi, N. Soga, N. Ishizuka and N. Tanaka, "Effect of domain size on the performance of octadecylsilylated continuous porous silica columns in reversed-phase liquid chromatography", Journal of Chromatography A, 1998, 797, 121-131.
6. P. D. Fletcher, S. J. Haswell, P. He, S. M. Kelly and A. Mansfield "Permeability of silica monoliths containing micro-and nano-pores", Journal of Porous Materials, 2011, 18, 501-508.
7. A. Storm, "Diamond: glittering prize for materials science", Science, 1990, 1640, 1643.
8. C. Mulder and J. Van Lierop, "Aerogels, Preparation, densification and characterization of autoclave dried SiO<sub>2</sub> gels" New York, Springer, 1986.
9. G. Pajonk, "Transparent silica aerogels", Journal of Non-Crystalline Solids, 1998, 225, 307-314.
10. L. Kocon, F. Despetis and J. Phalippou, "Ultralow density silica aerogels by alcohol supercritical drying", Journal of Non-Crystalline Solids, 1998, 225, 96-100.
11. M. Schneider and A. Baiker, "Aerogels in catalysis" Catalysis Reviews, 1995, 37, 515-556.
12. F. Schwertfeger, D. Frank and M. Schmidt, "Hydrophobic waterglass based aerogels without solvent exchange or supercritical drying" Journal of Non-Crystalline Solids, 1998, 225, 24-29.
13. Y. K. Akimov, "Fields of application of aerogels, Instruments and Experimental Techniques", 2003, 46, 287-299.
14. J. Randon, J. F. Guerrin and J. L. Rocca, "Synthesis of titania monoliths for chromatographic separations" Journal of Chromatography A, 2008, 1214, 183-186.
15. J. Randon, S. Huguet, A. Piram, G. Puy, C. Demesmay and J. L. Rocca, "Synthesis of zirconia monoliths for chromatographic separations", Journal of Chromatography A, 2006, 1109, 19-25.

16. I. U. Arachchige and S. L. Brock, "Highly luminescent quantum-dot monoliths" , Journal of The American Chemical Society, 2007, 129, 1840-1841.
17. M. Shafaei-Fallah, J. He, A. Rothenberger and M. G. Kanatzidis, "Ion-exchangeable cobalt polysulfide chalcogen" , Journal of The American Chemical Society, 2011, 133, 1200-1202.
18. B. Gaweł, K. Gaweł and G. Oye, "Sol-gel synthesis of non-silica monolithic materials, Materials" 2010, 3, 2815-2833.
19. K. Fujita, J. Konishi, K. Nakanishi and K. Hirao, " Strong light scattering in macroporous TiO<sub>2</sub> monoliths induced by phase separation", Applied Physics Letters, 2004, 85, 5595-5597.
20. L. Rieux, H. Niederländer, E. Verpoorte and R. Bischoff, "Silica monolithic columns: synthesis, characterisation and applications to the analysis of biological molecules", Journal of Separation Science, 2005, 28, 1628-1641.
21. H. Zou, X. Huang, M. Ye and Q. Luo, "Monolithic stationary phases for liquid chromatography and capillary electrochromatography", Journal of Chromatography A, 2002, 954, 5-32.
22. I. Nischang, I. Teasdale and O. Brüggemann, "Porous polymer monoliths for small molecule separations: advancements and limitations", Analytical and Bioanalytical Chemistry, 2011, 400, 2289-2304.
23. J. N. Kondo and K. Domen, "Crystallization of mesoporous metal oxides", Chemistry of Materials, 2007, 20, 835-847.
24. K. Nakanishi and N. Tanaka, "Sol-gel with phase separation. Hierarchically porous materials optimized for high-performance liquid chromatography separations", Accounts of Chemical Research, 2007, 40, 863-873.
25. A. Galarneau, J. Iapichella, K. Bonhomme, F. Di Renzo, P. Kooyman, O. Terasaki and F. Fajula, "Controlling the morphology of mesostructured silicas by pseudomorphic transformation: a route towards applications", Advanced Functional Materials, 2006, 16, 1657-1667.
26. E. C. Peters, F. Svec, J. M. Fréchet, C. Viklund and K. Irgum, "Control of porous properties and surface chemistry in "molded" porous polymer monoliths prepared by polymerization in the presence of TEMPO, Macromolecules", 1999, 32, 6377-6379.
27. N. Rupcich, R. Nutiu, Y. Li and J. D. Brennan, "Solid-phase enzyme activity assay utilizing an entrapped fluorescence-signaling DNA aptamer" , Angewandte Chemie, 2006, 118, 3373-3377.
28. Y. Chen, Y. Yi, J. D. Brennan and M. A. Brook, "Development of macroporous titania monoliths using a biocompatible method" , Chemistry of Materials, 2006, 18, 5326-5335.

29. E. Alzahrani and K. Welham, "Design and evaluation of synthetic silica-based monolithic materials in shrinkable tube for efficient protein extraction", *Analyst*, 2011, 136, 4321-4327.
30. K. Nakanishi and N. Soga, "Phase separation in silica sol-gel system containing polyacrylic acid", *Journal of Non-Crystalline Solids*, 1992, 139, 1-13.
31. D. Allen and Z. El Rassi, "Capillary electrochromatography with monolithic silica columns", *Journal of Chromatography A*, 2004, 1029, 239-247.
32. L. C. Klein, Boston. "Sol-gel optics: processing and applications", Kluwer Acad. Publ., 1994.
33. Rahman, Mohammed Shahidur. "Utilizing mixed surfactants for simultaneous pore templating and active site formation in metal oxides." (2009).
34. Smått, Jan-Henrik, Stephan Schunk, and Mika Lindén. "Versatile double-templating synthesis route to silica monoliths exhibiting a multimodal hierarchical porosity." *Chemistry of materials* 15.12 (2003): 2354-2361.
35. Smått, Jan-Henrik, et al. "Hierarchically porous metal oxide monoliths prepared by the nanocasting route." *Chemistry of materials* 18.6 (2006): 1443-1450.
36. Palmqvist, Anders EC. "Synthesis of ordered mesoporous materials using surfactant liquid crystals or micellar solutions." *Current opinion in colloid & interface science* 8.2 (2003): 145-155.
37. Cagnol, F.; Grosso, D.; Soler-Illia, G. J. d. A. A.; Crepaldi, E. L.; Babonneau, F.; Amenitsch, H.; Sanchez, C., Humidity-controlled meso structuration in CTAB-templated silica thin film processing. "The existence of a modulable steady state". *J. Mater. Chem.* 2003, 13, (1), 61-66.
38. Khattab, Amin Khalid "Fabrication, functionalization and characterization of silica monolith for forensic chemistry applications" Diss. University of Hull, 2014.
39. Linsebigler, A.L., G. Lu, and J.T. Yates Jr, "Photocatalysis on TiO<sub>2</sub> surfaces: principles, mechanisms, and selected results" *Chemical reviews*, 1995. 95(3): p. 735-758.
40. Chao, Zi-Sheng, and Eli Ruckenstein. "Effect of the nature of the templating surfactant on the synthesis and structure of mesoporous V-Mg-O." *Langmuir* 18.3 (2002): 734-743.